INTERNATIONAL JOURNAL OF CLIMATOLOGY
Int. J. Climatol. **34**: 3585–3603 (2014)
Published online 12 February 2014 in Wiley Online Library
(wileyonlinelibrary.com) DOI: 10.1002/joc.3931

RMetS
Royal Meteorological Society

Spatiotemporal patterns in the mean and extreme temperature indices of India, 1971–2005

Dileep K. Panda,[a]* A. Mishra,[b] A. Kumar,[a] K. G. Mandal,[a] A. K. Thakur[a] and R. C. Srivastava[a]

[a] *Directorate of Water Management (ICAR), Bhubaneswar, Odisha, India*
[b] *International Water Management Institute, Southern Africa Office, Pretoria, South Africa*

ABSTRACT: This study provides the comprehensive analysis of changes in mean and extreme temperature indices of India to assist the climate change mitigation and adaptation strategies and to add information for the global comparisons, using a high-resolution daily gridded temperature data set ($1^\circ \times 1^\circ$) during 1971–2005. In addition to the indices recommended by the World Meteorological Organization/CLIVAR Expert Team on Climate Change Detection and Indices, few more indices having social and agricultural implication are investigated at the seasonal and annual scales, utilizing widely adopted statistical methodologies in climate research. The results show, in general, a robust signal of warming, broadly consistent with what has been observed and predicted in other parts of the world in the context of global warming. The frequency and intensity of warm extremes, especially representing the daily minimum temperature, have increased with simultaneous decreases in cold extremes in large parts of the country, but the spatial distribution of the trend magnitude reflects the complex natural climatic settings of India and its possible interaction with the anthropogenic forcing. Seasonal analysis reveals a faster warming in day and night temperatures in winter affecting the major wheat crop. In summer, however, both human and ecosystems appear to be more vulnerable to the increasing tendency of the heatwave occurrences, particularly during night-time, since the 1990s. The relationship with the large-scale natural climatic modes indicates that the warming indices tend to increase in the year following the El Niño events as evident from the correlation with the NINO3.4 index, with a relatively higher association in the monsoon season. Moreover, the concurrent correspondence of the summer heatwaves with the north Indian Ocean sea surface temperature suggests a degree of predictability of the heat stress episode.

KEY WORDS extreme temperature indices; India; seasonality; ENSO; global warming; trends

Received 5 November 2013; Revised 11 December 2013; Accepted 26 December 2013

1. Introduction

The 20th century global warming with consequent occurrences in climate extremes is likely to increase in frequency and intensity in future, as highlighted in the successive Intergovernmental Panel on Climate Change (IPCC) assessment reports (IPCC, 2007; Field *et al.*, 2012). Observations of some of the recent studies have now become the subject of political and scientific attention, which point towards a climate-induced threat to the world's food, freshwater and biodiversity security (Vörösmarty *et al.*, 2010; Wheeler and von Braun, 2013). Signature of global warming and its adverse impacts on society and environment, through an accelerated hydrological cycle, is more reflected in extreme indices than in the mean states of climate (Easterling *et al.*, 2000). Therefore, numerous studies have been conducted at the global, continental and subcontinental scales (Alexander *et al.*, 2006; Klein Tank *et al.*, 2006; Brown *et al.*, 2008; Aguilar *et al.*, 2009; Caesar *et al.*, 2011; You *et al.*, 2011; Vincent *et al.*, 2011; Donat *et al.*, 2013a, 2013b; Santo *et al.*, 2013). In particular, most of these studies have been carried out with the special initiative of the World Meteorological Organization (WMO) Joint Expert Team on Climate Change Detection and Indices (ETCCDI) through the international collaborations for the development of extreme indices and high-resolution data sets (Peterson and Manton, 2008).

Consistent with the warming-induced changes in climate and ecosystems over large parts of the world, the Indian subcontinent has been witnessing the adverse impacts of global warming in recent decades. In particular, the monsoon rainfall, which is fundamentally generated from a thermal contrast between land and ocean, has shown large variability in terms of frequency and intensity of extreme events (Goswami *et al.*, 2006; Krishnamurthy *et al.*, 2009; Jhajharia *et al.*, 2012). This has adversely affected the Indian agriculture, which is the backbone of the country's economy by ensuring livelihood security to its over 1.2 billion populations (Krishna Kumar *et al.*, 2011; Auffhammer *et al.*, 2012). Moreover, the ecosystems and the densely populated urban establishments along the coastal track have been vulnerable to the warming-induced sea level rises from the snow and glacier melting over the northern Himalayan river basins, and that from coastal surges of the severe

* Correspondence to: D. K. Panda, Directorate of Water Management (ICAR), Chandrasekharpur, Bhubaneswar 751023, Odisha, India.
E-mail: dileeppanda@rediffmail.com

cyclonic storm and hurricane over the north Indian Ocean (Hoyos *et al.*, 2006; Unnikrishnan and Shankar, 2007; Bolch *et al.*, 2012). The projected future warming over India suggests that the monsoon climate will intensify with more droughts and heat stress, which could result in food and water crisis, given the burgeoning population (May, 2011; Wheeler and von Braun, 2013; World Bank, 2013).

Most of the previous studies in India have used the seasonal and annual mean of daily maximum (T_{max}), minimum (T_{min}), mean (T_{mean}) temperatures and diurnal temperature range (DTR $= T_{max} - T_{min}$) data sets, showing an asymmetric nature of change in T_{max} and T_{min} at both the spatial and temporal scales. During the last century, the observed warming in annual T_{mean} has been due to the significant increases in T_{max}, as T_{min} remained non-significant or neutral, leading to an increasing pattern in DTR (Rupa Kumar *et al.*, 1994; Kothawale and Rupa Kumar, 2005; Fowler and Archer, 2006). However, the reported warming in most parts of the world has been due to the larger contribution from T_{min} in comparison with T_{max}. In India, T_{mean} has experienced an accelerated warming since the 1970s, characterized by significant increases in both T_{max} and T_{min} (Kothawale *et al.*, 2010).

In recent years, the extreme states of day and night temperatures in India have caused adverse impacts on the major crops through changes in phenological development and physiological processes. Rice and other cereals showed a reduction in yield when T_{min} increased beyond a threshold limit (Welch *et al.*, 2010), consistent with the findings of Peng *et al.* (2004). Similarly, a significant acceleration of wheat senescence, an important limitation to grain filling, was observed when temperature exceeded 34 °C in winter, with consequent yield losses in the intensely grown wheat belt of India (Lobell *et al.*, 2012). Notably, the Indian subcontinent is one of the global hot spots of heat stress on agricultural crops (Teixeira *et al.*, 2013). Moreover, the heat and cold waves have increased in recent years (De and Mukhopadhyay, 1998; Pai *et al.*, 2004). Nevertheless, there have been fewer studies to evaluate the changes in extreme indices of daily temperatures (Revadekar *et al.*, 2009; Dash and Mamgain, 2011) in spite of the fact that they provide key indication of different aspects of climate change with social and economic relevance in India. It should also be mentioned that in the recent global and continental scale studies, the Indian subcontinent has been inadequately represented because of the lack of well-calibrated data sets (Alexander *et al.*, 2006; Klein Tank *et al.*, 2006; Brown *et al.*, 2008; Caesar *et al.*, 2011; Perkins *et al.*, 2012). A recent special report by IPCC also highlighted that data gaps in many parts of the globe, including India, leads to limitations in understanding the changes in climate extremes (Field *et al.*, 2012).

The primary focus of this study is to identify and quantify the changes in mean and extreme temperature indices during the period 1971–2005 by using the robust statistical tools. To this end, a high-resolution daily gridded temperature data set at $1^\circ \times 1^\circ$ resolution (Srivastava *et al.*, 2009) is used to calculate the ETCCDI-defined indices that are relevant to the Indian climatology. As the mean and extreme temperature indices exhibit strong warming trends since the early 1970s at the global and national scales (IPCC, 2007; Morek *et al.*, 2013), this study period here is less likely to be influenced by the trends of the preceding cooling phase of the last century. In contrast to the regional patterns identified by Dash and Mamgain (2011), this study assesses the grid scale trends and also maps their magnitudes to understand the spatial variability at high resolution in different seasons. In addition, we investigate the changes in the degree-day (DD) and in the degree-night (DN) indices representing the frequency and magnitude of day- and night-time heatwaves (Gershunov *et al.*, 2009), as there has been a growing heat-wave-induced human causalities in recent decades (De *et al.*, 2005). To further understand the heat-induced yield losses in India (Lobell *et al.*, 2012), changes in the heat stress intensity (HSI) index during the winter season is also explored (Teixeira *et al.*, 2013). Finally, the influence of the large-scale climatic modes, such as the El Niño-Southern Oscillation (ENSO) and the north Indian sea surface temperature (SST), is examined, since they modulate the temperature extremes globally and also that of the Indian subcontinent (Revadekar *et al.*, 2009; Arblaster and Alexander, 2012; Trenberth and Fasullo, 2012). Analysis of the high-resolution data set is expected to improve the adaptation and mitigation strategies, given the fact that the Indian subcontinent is one of the largest emitter of the greenhouse gases.

2. Data and methods

2.1. Gridded data set and extreme indices

This study is based on the high-resolution daily gridded temperature data set at $1^\circ \times 1^\circ$ resolution, which is developed by the Indian Meteorological Department (IMD) using temperature data of 395 quality-controlled stations (Srivastava *et al.*, 2009). The station data were interpolated into grids using the modified version of the Shepard's (1968) angular distance weighting algorithm, an interpolation technique that was previously used by New *et al.* (2000), Kiktev *et al.* (2003) and Caesar *et al.* (2006) for developing gridded temperature data set. The root mean square error (RMSE) was estimated for cross-validation and found to be less than 0.5 °C for most parts of the country, with little exception over the northern top. This data set was subjected to a comprehensive set of quality assurance procedures, particularly to check the possibility of artificial trends from stations of different record length and stations, and found highly correlated with other global gridded data sets (Srivastava *et al.*, 2009). Moreover, Dash and Mamgain (2011) observed that this data set is homogeneous in space and time, which has been used for the validation of climate model simulation and trend analysis (Pingale *et al.*, 2014).

This study uses the daily maximum (TX) and minimum (TN) temperatures recorded over 329 grid points representing the whole country during 1971–2005. Considering the agricultural and societal implication of the mean and extreme temperature indices, analysis is carried out for both the seasonal and annual scales. Based on the Indian nomenclature, the summer season (March to May, MAM), internationally known as the boreal spring, is the warmest period characterized by the occurrence of heatwaves, while temperatures of the monsoon season (June to September, JJAS), internationally known as the summer, influence the predominant agriculture production of the country. The coldest period is boreal winter (December to February, DJF), during which wheat, fruits and vegetables are grown.

We mostly focus on the extreme temperature indices recommended by the WMO/CLIVAR ETCCDI (available from http://cccma.seos.uvic.ca/ETCCDI). In order to compare the changing climate of different regions of the world and also to validate the climate model simulations, these indices have been developed in the course of time that represents diverse aspects of extreme temperature in terms of intensity, frequency and duration (Peterson and Manton, 2008; Zhang *et al.*, 2011). Definitions of all these indices are given in Table 1. While some of the ETCCDI indices, such as the number of frost days (FD) and growing season length (GSL), are not relevant for the Indian climate both in spatial and in seasonal context, others like summer days over 25 °C (SU25) and tropical nights (TR20) do not match the threshold for some seasons. Therefore, we use additional locally defined thresholds, such as the summer days over 30/40 °C (SU30/SU40). According to Alexander *et al.* (2006), these indices can be grouped into different categories, such as the absolute extreme indices, percentile-based indices, threshold indices and duration indices. Although the absolute and threshold-based indices are useful for impact assessment and regional planning, the percentile-based indices have relative advantage for climate change detection studies and for comparison over a diverse climate (Klein Tank and Können, 2003).

Although the spell-based temperature indices [i.e. cold spell duration index (CSDI) and warm spell duration index (WSDI)] provide important information and also validate the occurrence of other extremes, they are less effective to capture the heatwave frequency and intensity, for the very reason that the six consecutive days over the 90th percentile is less observed (Perkins and Alexander, 2013). We, therefore, use the DD and DN heatwave indices for the summer season which capture the hottest 1% temperature for a duration of at least one, two or three consecutive days or nights (Gershunov *et al.*, 2009). Because, a heatwave spell of two consecutive days can significantly increase the human mortality risk (Shakoor *et al.*, 2005). In general, the DD indices are important indicators of climate change (You *et al.*, 2013a). Moreover, it is reported that wheat production in India, the third largest producer of the world, has experienced serious challenges due to extreme temperatures in recent years (Lobell *et al.*, 2012). Thus, the HSI index defined by Teixeira *et al.* (2013) has been used to assess the vulnerability of the winter wheat.

2.2. Statistical methodology

We use two well-established statistical procedures to test whether the temperature time series are non-stationary (i.e. presence of trends) and to evaluate the magnitude of non-stationarity. First, the nonparametric Mann–Kendall test is used for the detection of monotone trends, which has been applied frequently in analysing environmental and climate data sets (Hipel and McLeod, 2005; Chandler and Scott, 2011). The advantage of this test is that it does not make any assumption about the distribution of the data, and also is capable of handling the outlying observations, generally observed in the extreme indices, under the assumption that data are independently distributed in time. Second, it is also important to assess the rate of changes over the study period, which has been carried out by using the nonparametric Kendall's slope estimator for trend quantification (Sen, 1968). A number of recent studies that have assessed the changes in climatic variables using these procedures include Alexander and Arblaster (2009), Aguilar *et al.* (2009), Caesar *et al.* (2011), You *et al.* (2011) and Dinpashoh *et al.* (2013). Analysis has been carried out for both the seasonal and annual scales. Significance of the trends is assessed at the 0.05 and 0.1 levels ($p \leq 0.05$ and $p \leq 0.1$), but the significant trends at the 0.05 level ($p \leq 0.05$) are mapped and interpreted (unless mentioned otherwise). Furthermore, the inverse distance weighted method (Daly, 2006) is used to interpolate the trend magnitudes.

Among the large-scale atmospheric patterns that drive internal variability in the climatic system, the ENSO and the north Indian SST influence the inter-annual variability of the seasonal temperature in India (Chowdary *et al.*, 2013). To investigate their relationships with extreme temperature indices, the Spearman's rank correlation is used. From the NOAA Extended Reconstructed Sea Surface Temperature Version 3 (ERSST.v3b) data set (Smith *et al.*, 2008), the NINO3.4 index that represents the ENSO is derived by averaging the SST anomalies over the Niño 3.4 region (5°N–5°S, 120°W–170°W), while the north Indian SST is derived by averaging the SST anomalies over 10–25°N and 50–100°E encompassing the Arabian Sea and Bay of Bengal. Before computing the correlation coefficients, the indices are de-trended. Using the probability density functions (PDFs), a comparison has also been made to understand the changes in the mean and extreme temperature indices between the El Niño (i.e. 1972, 1977, 1982, 1987, 1991, 1992, 1997 and 2002) and La Niña (i.e. 1970, 1971, 1973, 1975, 1988 and 1999) years (Halpert and Ropelewski, 1992; Kothawale *et al.*, 2008). Moreover, the recent changes in the distribution of extreme indices are discussed by comparing the PDFs for the pre-1990 (1971–1989) and post-1990 (1990–2005) periods.

Table 1. Definition of the ETCCDI and other relevant temperature indices used in this study.

Index (unit)	Description	Definition
T_{max} (°C)	Mean daytime temperature	Seasonal or annual mean of daily maximum temperature (TX)
T_{min} (°C)	Mean night-time temperature	Seasonal or annual mean of daily minimum temperature (TN)
T_{mean} (°C)	Mean average temperature	Seasonal or annual mean of daily average of TX and TN
TXx (°C)	Warmest day	Seasonal or annual highest of TX
TNx (°C)	Warmest night	Seasonal or annual highest of TN
TXn (°C)	Coldest day	Seasonal or annual lowest of TX
TNn (°C)	Coldest night	Seasonal or annual lowest of TN
TX90p (%)	Warm day frequency	Percentage of days when TX >90th percentile of the 1971–1990 baseline period
TN90p (%)	Warm night frequency	Percentage of days when TN >90th percentile of the 1971–1990 baseline period
TX10p (%)	Cold day frequency	Percentage of days when TX <10th percentile of the 1971–1990 baseline period
TN10p (%)	Cold night frequency	Percentage of days when TN < 10th percentile of the 1971–1990 baseline period
DTR (°C)	Diurnal temperature range	Seasonal or annual mean difference between TX and TN
SU25, SU30, SU40	Summer days	Seasonal or annual count of days when TX >25, 30 and 35 °C
TR20 (days)	Tropical nights	Seasonal or annual count of days when TN >20 °C
WSDI (days)	Warm spell duration indicator	Seasonal or annual count of days with at least six consecutive days when TX >90th percentile
CSDI (days)	Cold spell duration indicator	Seasonal or annual count of days with at least six consecutive days when TN <10th percentile
$DD_{99}F$ (n) (days)	Degree-day heatwave frequency	Summer season count of days with at least $n = 1$, 2 or 3 consecutive days when TX >99th percentile
$DN_{99}F$ (n) (days)	Degree-night heatwave frequency	Summer season count of days with at least $n = 1$, 2 or 3 consecutive days when TN >99th percentile
$DD_{99}M/DN_{99}M$ (°C)	Degree-day/night heatwave magnitude	Summer season sum of the exceedance temperature when TX/TN >99th percentile
HSI	Heat stress intensity index	The daily values of HSI is 0 if $T_{max} < T_{crit}$ [T_{crit} is the threshold temperature above which yield damage resumes during the thermal-sensitive period (TSP) of wheat], and $(T_{max} - T_{crit})/(T_{lim} - T_{crit})$ if $T_{crit} \leq T_{max} < T_{lim}$ and 1 if $T_{max} \geq T_{lim}$. The average over the TSP is calculated to represent the seasonal HSI, with $T_{crit} = 27$ °C and $T_{lim} = 40$ °C for wheat crop

TX is the daily maximum temperature; TN is the daily minimum temperature.

3. Results and discussion

3.1. Changes in mean temperature

Figure 1 displays the spatial distribution of daily maximum (daytime TX) and minimum (night-time TN) temperatures averaged over the period 1971–2005, while Figure 2 shows the inter-annual variability of the nationally averaged time series at the seasonal and annual scales, reflecting the diverse climatology of the Indian subcontinent. Despite the occurrence of the warm and cold years in terms of a large inter-annual variability, the nationally averaged night-time temperatures (T_{min}) shows a significant ($p \leq 0.05$) increasing trend of about 0.15 °C decade^{-1} in winter and summer, compared with a non-significant increase in the corresponding daytime temperature (T_{max}) at a rate of 0.07 and 0.11 °C decade^{-1}, respectively (Figure 2). At the annual scale, T_{min} also display a significant warming trend of 0.11 °C decade^{-1}, while T_{max} reflects the pattern of the summer season. As the monsoon season T_{max} and T_{min} show no obvious tendency (Figure 2), it can be inferred that the annual pattern of T_{min} is due to winter T_{min}. Furthermore, the average of daytime and night-time temperature (T_{mean}) in winter and summer depicts more the pattern of T_{min} than that of T_{max}. Overall, these results are consistent with the reported warming at the global and regional scales considering different time frames since the 1950s (Easterling *et al.*, 1997; Vose *et al.*, 2005; IPCC, 2007).

Figure 3 shows the grid-scale spatial pattern of trends in T_{max}, T_{min} and T_{mean} during 1971–2005 for the summer (S), monsoon (M) and winter (W) seasons and annual (A) scales. Although the frequency of the increasing trends in mean daytime (T_{max}) and night-time temperatures (T_{min}), which outnumber the corresponding decreasing trends in high proportion, is similar in summer and monsoon, the warming patterns in T_{min} are stronger with more significant ($p \leq 0.05$) trends compared with those in T_{max} (Table 2 and Figure 3). In winter, the frequency and magnitude of warming trends in T_{max}, T_{min} and T_{mean} show clear increases over those of the other two seasons. Moreover, it is interesting to note the contrasting spatial orientation of the daytime and night-time significant warming trends in winter; while T_{max} has decreased in the northern Indo-Gangetic region,

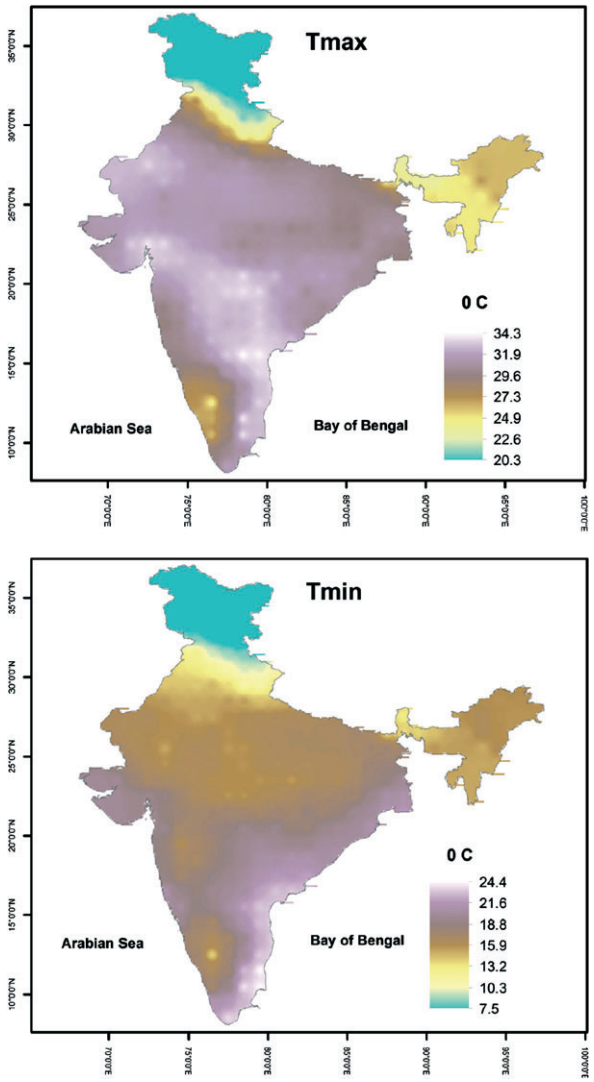

Figure 1. Spatial distribution of the daily maximum (T_{max}) and minimum (T_{min}) temperatures averaged over the period 1971–2005.

T_{min} has decreased in the eastcentral and central parts of India (Figure 3). It should also be noted that the spatial distribution of trends in the mean temperature (T_{mean}) is consistent with that in T_{max} and T_{min} in winter and annual scales only, whereas the summer and monsoon season warming in T_{min} is less captured in T_{mean}. In addition, the annual trends in T_{max}, T_{min} and T_{mean} are contributed by the winter trends as evident from the similarity in spatial distributions, while the other two seasons are noticeably less manifested. Moreover, the monsoon season increases in T_{max} and T_{min} (Figure 3) have not been captured in the nationally averaged time series, possibly because of the large spatial and temporal variability (Figure 2).

Although the Indian subcontinent is considered climatologically tropical, the complex spatial and seasonal differences observed in the mean day- and night-time temperatures, consistent with the findings of the basin scale studies (Bhutiyani *et al.*, 2007; Singh *et al.*, 2008; Jhajharia *et al.*, 2013), underscore the need of understanding the swings in their extreme indices.

3.2. Changes in extreme temperature indices

3.2.1. Changes in warm extremes

The temperatures of warmest days (TXx) and nights (TNx) show a general warming trend in terms of frequency and occurrence over many parts of the country, with relatively stronger trends observed in TNx in summer and winter (Table 2 and Figure 4). It is, however, interesting to see the contrasting spatial delineation of the significant trends in different seasons. In summer and winter, the maximum daytime temperatures (TXx) are increasing significantly in the southern, central and westcentral parts of India, while the maximum night-time temperatures (TNx) are increasing significantly in north and northeast India; in the monsoon season, however, significant warming in TNx is observed over the south and westcentral India. The nationally averaged TXx and TNx indicate that the summer and winter TXx have increased non-significantly at a rate of about 0.12 °C decade^{-1} in comparison with a significant ($p \leq 0.1$) decadal increase of 0.22 °C in winter TNx. Consistent with the absolute extreme indices TXx and TNx, the percentile-based frequency of warm days (TX90) and warm nights (TN90) also show a predominance of increasing trends, particularly the significant increases of TN90 in most parts of the country in monsoon, winter and annual scales. In winter, notably, both TX90 and TN90 are increasing at a faster rate with the spatial congregation of significant trends over a large domain, leading to a country-wide significant increase of about 1.5% of days in a year per decade.

The threshold-based warming indices, such as the summer days over 25, 30 and 40 °C (SU25, SU30, SU40), do not provide any clear signal of change as that of the absolute- and percentile-based indices (Table 2). For SU25, most of the days of summer and monsoon season exceed the threshold temperature of 25 °C, while the winter and annual trends indicate a tendency towards warmer climate. In summer, however, SU30, which is the indicator of hot days in north India, show non-significant increases over large parts of the country. SU40, a relevant indicator of the summer hot days in south and central India, also exhibits the occurrence of more increasing trends. The non-significance of trends in SU30 and SU40 for both the grid-scale and nationally averaged time series (Figure 5(a)) is possibly due to the large inter-annual variability. However, the occurrence of such events in terms of positive anomaly might have led to mortality risk, as reported in the megacities of the world (Shakoor *et al.*, 2005). The frequency of trends in tropical night (TR20) suggests that, in summer and annual time series, there are indications of warming patterns, with considerable similarity to that of the TNx and TN90p trends (Figure 4). In monsoon and winter, however, most of the time series appear to fall short of the threshold value, although the frequency of trends indicates an increased occurrence of the warming patterns, with no conspicuous pattern in the national average.

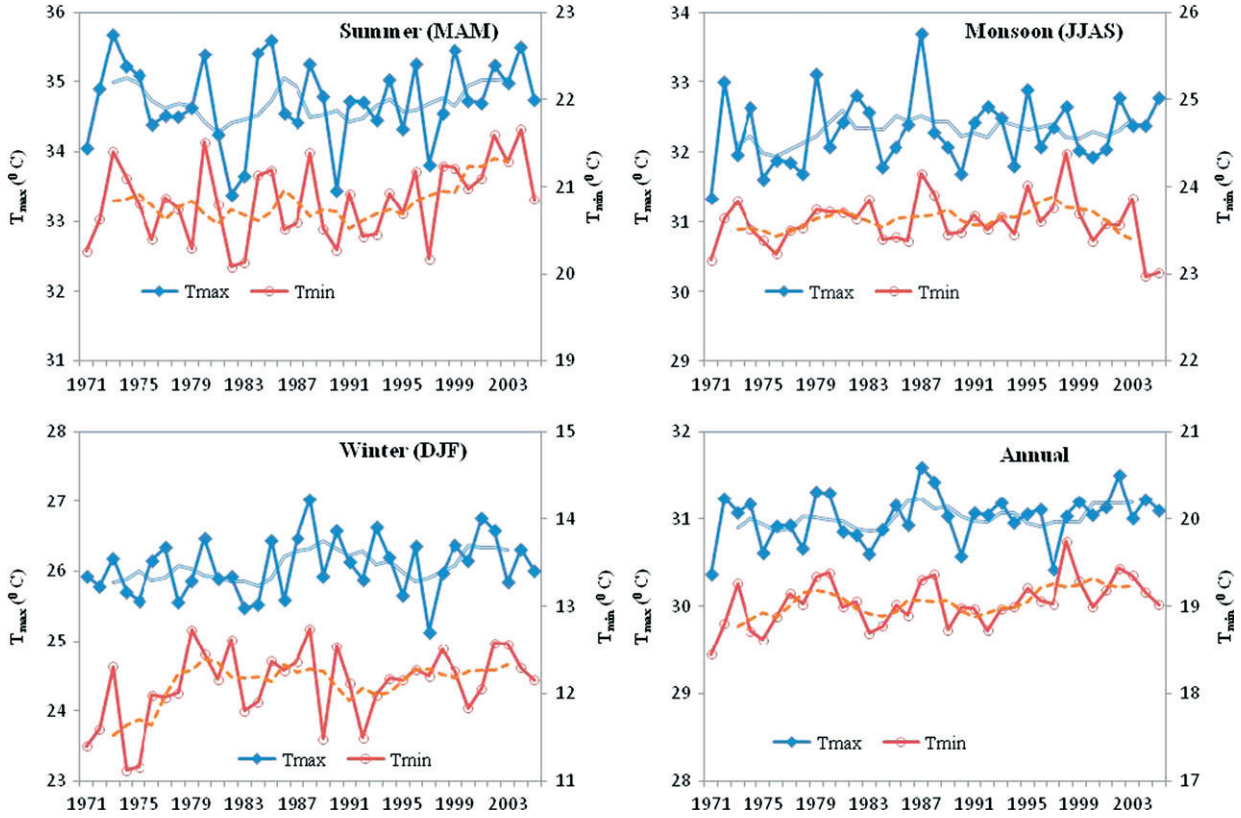

Figure 2. The nationally averaged seasonal and annual mean of daily maximum (T_{max}) and daily minimum (T_{min}) temperature during 1971–2005. The inscribed solid and dotted lines indicate the 5-year moving average for T_{max} and T_{min}, respectively.

WSDI in winter indicates the occurrence of a large number of increasing trends across the country (not shown), except some patches along the northeast coast (Table 2). But, significant trends are very less, which are observed along the westcoast tract, similar to the spatial orientation of the annual WSDI (Table 2 and Figure 4(d)). In summer and monsoon, it shows a mixture of increasing and decreasing trends with few significant trends, possibly due to the large inter-annaul variability as observed in the nationally averaged WSDI (not shown). Although the country-wide WSDI displays the non-significant increases, it is worthwhile to mention the increase in the warm spell duration at a rate of 10.5 days decade^{-1} in winter.

However, clear signals of increases in heatwaves of the summer season are evident from the trends in DD (DN) heatwave frequency DD99F (DN99F) (Table 2 and Figure 4(a)), which is not captured in the daytime warm spells (i.e. WSDI). In particular, the summer nights have experienced widespread increases in heatwaves frequency and magnitude, as evident from the DN heatwave frequency/magnitude of one day (i.e. DN99F/DN99M), spatially consistent with the other night-time warming indices (i.e. TNx, TN90p and TR20). The frequency of increasing trends in DD/DN heatwave frequency for two and three consecutive days, DD99F (2,3)/DN99F (2,3), is similar to that of one-day frequency (i.e. DD99F and DN99F), but with fewer significant trends (Table 2). Although all the nationally averaged heatwave indices display a general rising pattern, the DN99F, DN99F (2) and DN99F (3) indices have increased significantly, suggesting that the night-time warming is more conspicuous than the daytime warming (Figure 5). However, it should be noted that the unusual years of an extended heatwave spell in Figure 5 (i.e. 1973, 1988 and 1998) have claimed about 1000 human population with a highest death tool of 1550 in 1998 (De *et al.*, 2005). The 1998 heatwave has also caused deaths in different parts of the world following the big 1997–1998 El Niño event (Füssel, 2009; Perkins *et al.*, 2012).

The observed frequencies in high temperatures of extended periods (i.e. WSDI) and the heatwave frequency indices would not necessarily coincide with other warm extremes discussed previously. However, a direct correspondence would confirm in part the cause of the warm extremes, as Perkins and Alexander (2013) observed that the increases in Australian warm indices are associated with an increasing frequency and intensity of some measures of heatwaves. In India, we also find that the summer TXx, TNx, TX90, TN90 and WSDI have strong associations with all the DD and DN heatwave indices, with significant ($p \leq 0.01$) correlation coefficients (R) ranging between 0.71 and 0.92. However, SU40 has a comparatively weaker association with the heatwave indices with an average correlation coefficient of 0.6 ($p \leq 0.01$) over the rest of the warm extremes including the WSDI. This

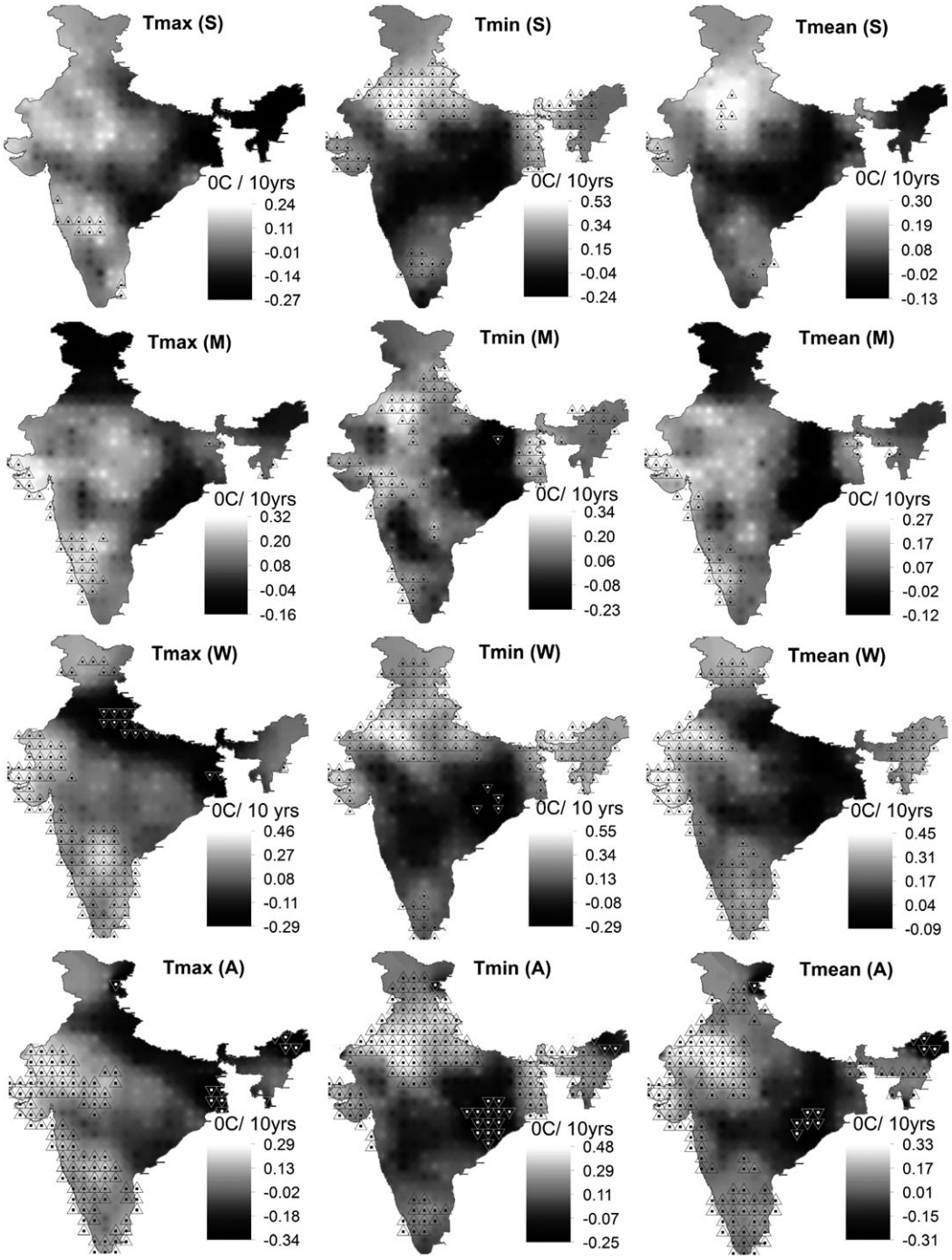

Figure 3. The spatial pattern of trends (°C decade^{-1}) in mean maximum (T_{max}), minimum (T_{min}) and average (T_{mean}) temperatures in summer (S, MAM), monsoon (M, JJAS), winter (W, DJF) and annual (A) time scales during 1971–2005. Significant ($p \leq 0.05$) positive/negative trends are shown as up/down triangles.

suggests that a considerable proportion of the trend and variability in summer warm extremes is explained by the heatwave indices, consistent with the findings of Perkins and Alexander (2013).

3.2.2. *Changes in cold extremes*

The trend results indicate that the cold extremes have exhibited the tendencies that are generally consistent with what one would expect based on the observed changes in warm extremes (Table 2 and Figure 4). The coldest day temperature (TXn) has increased substantially in summer and monsoon, with the significant monsoon warming trends over the northeastern, northcentral and extreme southwest parts of India (Figure 4(a) and (b)). It is, however, interesting to find the congregation of significant decreasing trends in the Indo-Gangetic north India and also in the parts of central India in the winter and annual scale (Figure 4(c) and (d)). These decreases could be due to the winter season surface cooling effects of the absorbing aerosols over the Indo-Gangetic Basin (Krishnan and

Table 2. Frequency of increasing (significant at $p \leq 0.05$ and $p \leq 0.1$ levels) and decreasing trends (significant at $p \leq 0.05$ and $p \leq 0.1$ levels) in mean and extreme temperature indices observed from 329 grid boxes during 1971–2005.

Index	Summer (MAM)		Monsoon (JJAS)		Winter (DJF)		Annual	
	Positive	Negative	Positive	Negative	Positive	Negative	Positive	Negative
T_{max}	221 (11, 22)	104 (1, 5)	257 (35, 51)	67 (0, 0)	249 (106, 127)	76 (18, 28)	232 (101, 125)	92 (15, 17)
T_{min}	259 (106, 130)	70 (0, 2)	272 (83, 119)	57 (1, 3)	264 (148, 163)	62 (4, 7)	254 (146, 166)	73 (20, 26)
T_{mean}	256 (14, 38)	68 (0, 0)	277 (39, 68)	45 (0, 0)	295 (132, 153)	32 (0, 0)	274 (131, 185)	54 (13, 18)
TXx	229 (44, 75)	98 (3, 9)	178 (2, 14)	148 (29, 43)	219 (47, 81)	106 (7, 12)	212 (58, 87)	115 (5, 11)
TNx	219 (65, 90)	108 (1, 2)	192 (32, 46)	132 (17, 33)	275 (64, 88)	52 (3, 4)	198 (44, 63)	127 (3, 8)
TXn	246 (3, 17)	77 (0, 0)	224 (41, 70)	96 (0, 0)	127 (3, 9)	198 (36, 51)	121 (9, 17)	202 (35, 49)
TNn	295 (103, 142)	30 (0, 0)	278 (42, 71)	51 (0, 0)	254 (109, 140)	74 (5, 10)	257 (110, 141)	71 (5, 10)
TX90p	210 (27, 47)	110 (17, 24)	172 (11, 30)	152 (0, 16)	263 (77, 96)	60 (0, 2)	176 (25, 54)	150 (12, 13)
TN90p	240 (40, 78)	86 (0, 0)	225 (72, 99)	100 (6, 15)	261 (104, 135)	65 (1, 1)	217 (111, 124)	111 (5, 13)
TX10p	49 (0, 0)	278 (2, 12)	53 (0, 0)	273 (51, 86)	160 (46, 63)	166 (54, 65)	71 (3, 5)	257 (91, 133)
TN10p	59 (0, 1)	269 (98, 119)	63 (21, 22)	265 (100, 130)	84 (13, 21)	245 (115, 147)	62 (9, 12)	263 (121, 141)
DTR	133 (15, 25)	192 (85, 106)	175 (30, 55)	148 (28, 37)	155 (34, 51)	167 (97, 105)	185 (64, 92)	143 (76, 89)
SU25	163 (0, 2)	48 (0, 0)	111 (9, 11)	68 (0, 1)	195 (16, 34)	100 (7, 10)	237 (24, 52)	86 (5, 8)
SU30	244 (0, 9)	79 (0, 0)	N/A	N/A	N/A	N/A	N/A	N/A
SU40	147 (4, 7)	89 (5, 7)	N/A	N/A	N/A	N/A	N/A	N/A
TR20	217 (28, 49)	104 (3, 5)	169 (23, 28)	82 (6, 11)	84 (11, 15)	53 (0, 0)	208 (46, 75)	120 (14, 21)
WSDI	192 (4, 17)	136 (4, 7)	181 (6, 13)	142 (0, 3)	266 (29, 60)	59 (0, 0)	189 (24, 31)	132 (2, 6)
CSDI	77 (0, 0)	246 (13, 40)	82 (6, 10)	243 (25, 44)	60 (0, 0)	264 (4, 13)	147 (6, 18)	176 (15, 31)
$DD_{99}F$	186 (11, 22)	136 (1, 3)	N/A	N/A	N/A	N/A	N/A	N/A
$DN_{99}F$	222 (50, 74)	104 (1, 2)	N/A	N/A	N/A	N/A	N/A	N/A
$DD_{99}M$	187 (13, 29)	141 (1, 4)	N/A	N/A	N/A	N/A	N/A	N/A
$DN_{99}M$	233 (12, 32)	93 (0, 0)	N/A	N/A	N/A	N/A	N/A	N/A
$DD_{99}F$ (3)	168 (0, 1)	158 (0, 0)	N/A	N/A	N/A	N/A	N/A	N/A
$DN_{99}F$ (3)	234 (1, 12)	63 (0, 0)	N/A	N/A	N/A	N/A	N/A	N/A
HSI	N/A	N/A	N/A	N/A	230 (102, 125)	75 (0, 0)	N/A	N/A

Ramanathan, 2002; Dey and Tripathi, 2008). Nationwide, TXn shows a non-significant warming trend of 0.3 and 0.1 °C decade^{-1} in summer and monsoon, respectively, compared with a non-significant cooling trend of about 0.1 °C decade^{-1} in winter and annual TXn. This coincides with the aerosol-induced cooling trend of 0.3 °C during the last three decades since the 1970s (Krishnan and Ramanathan, 2002). The cold day frequency (TX10p), consistent with the patterns in TXn, has decreased with considerable spatial similarity *albeit* opposite trends. However, the decrease in the monsoon and annual TX10p has been widespread (Figure 4(b) and (d)), thus leading to a nationwide significant decreasing trend of about 1% of days in a year per decade. Notable is the significant increases in winter TX10p over the Indo-Gangetic north Indian belt, coinciding with the decreases in TXn.

The increases in the coldest night temperature (TNn) have been more pronounced than those in the TXn index in all the seasons, with relatively more significant warming trends in summer and winter scattered over large parts of the country except the eastern and southern parts, driving a similar pattern also in the annual TNn (Table 2 and Figure 4). This has led to a significant nationwide trend of 0.4, 0.2 and 0.2 °C decade^{-1} in the summer, winter and annual scales, respectively. Consistently, we find the large scale decreases in the cold night frequency (TN10p), whereas the north and northeast India have experienced significant declining trends at both the seasonal and annual scales. But, the nationally averaged summer and winter TN10p exhibit a significant downward trend of 1.1% of days in a year per decade. It is worthwhile to mention that the decrease in the frequency of cold nights (TN10p) is faster than the increase in the frequency of warm nights (TN90p) (Table 2), leading to a narrowing of the temperature distribution, as recently observed by Donat *et al.* (2013b) for the Arabian region. In general, this asymmetric change has decreased the variance of the temperature distribution in the northern hemisphere extra-tropics in contrast to an increase in low latitude during the past 60 years (Donat and Alexander, 2012).

CSDI indicates the prevalence of decreasing trends in large parts of the country irrespective of seasons (Table 2 and Figure 4), confirming a general increase in the daily minimum temperature, although the observed tendency in TNn and TN10p do not necessarily lead to a corresponding decrease in CSDI. Moreover, the spatial distribution of CSDI trends correspond well with that of TN10p through the same trend sign, and with that of the TNn, WSDI and the summer DN heat spell indices [$DN_{99}F$, $DN_{99}F$ (2,3)] through the opposite trend sign (Figure 4). While the trends in WSDI could not fully capture the patterns in daytime warming indices, relatively large decreasing trends in CSDI corroborates the clear signals of a faster night-time warming, and thus validates the simulated climate model prediction of an intense night-time temperature (Rupa Kumar *et al.*, 2006). Indeed, the globally averaged extreme indices of minimum temperature are also warming at a faster rate than the corresponding maximum temperature extremes

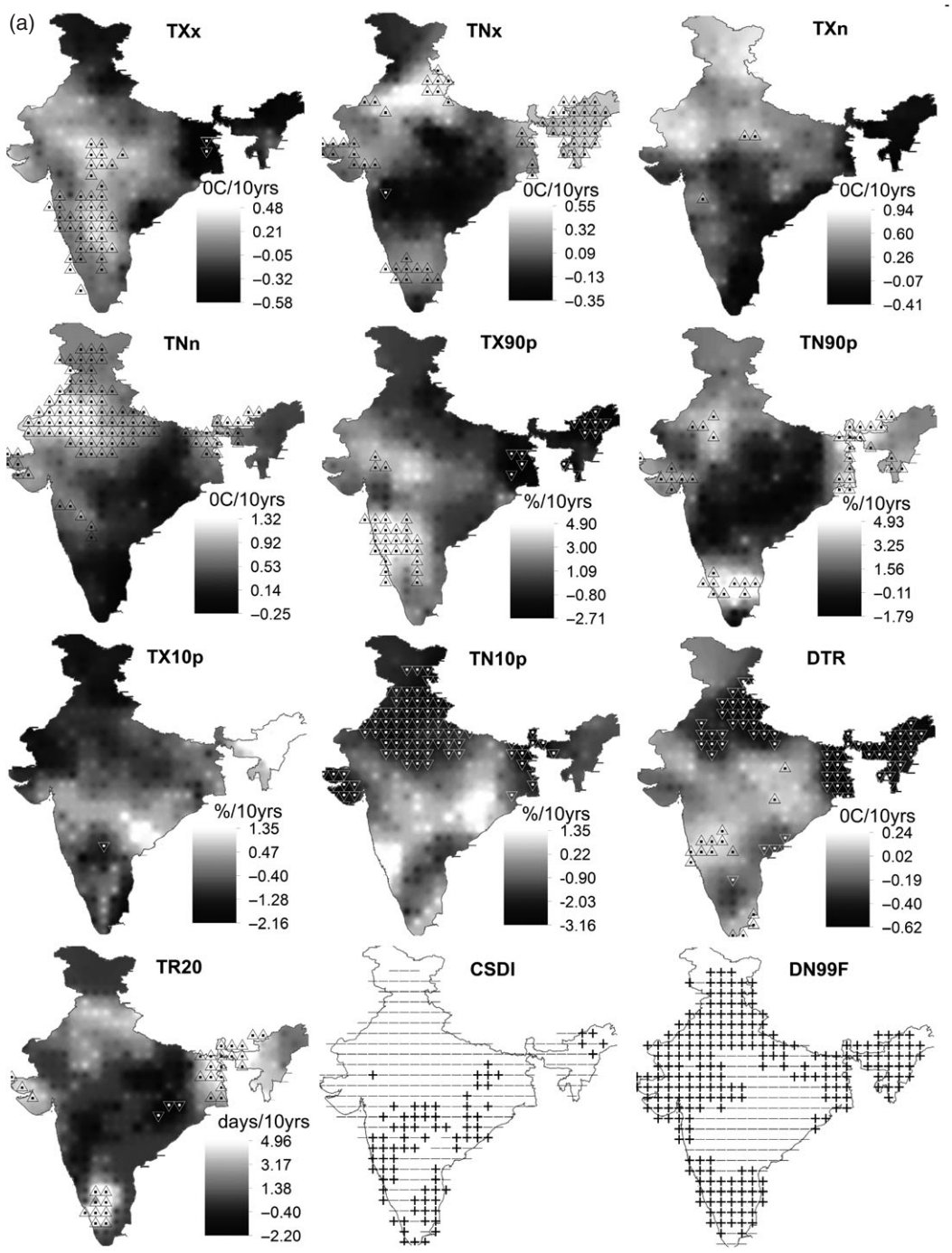

Figure 4. The spatial pattern of trends (per decade) in extreme temperature indices in (a) summer, (b) monsoon, (c) winter and (d) annual time scales during 1971–2005. Significant ($p \leq 0.05$) positive/negative trends are shown as up/down triangles. For CSDI and DN99F, the positive and negative trends are denoted by plus (+) and minus (−) signs, respectively.

(Donat *et al.*, 2013a). It is reported that changes in the surface characteristics and the boundary layer atmospheric constituents may be responsible for the relatively rapid increase in $T_{\min}$ (Christy *et al.*, 2008).

Indeed, Perkins and Alexander (2013) noted that the ETCCDI indices regarding hot temperature extremes were deemed inappropriate when concerning the measurement of heatwaves; in particular, the six consecutive days above the 90th percentile which define WSDI and CSDI are rarely identified, while a spell of half of this length can have impacts on many different sectors. Consistently, we observe that the spell-based indices (i.e. CSDI and WSDI) and also the threshold-based indices (i.e. SU25, SU30 and SU40) do not reflect the growing heat and cold waves which led to the adverse impacts on the human society and agriculture sector in India (Pai *et al.* 2004; De *et al.*, 2005; Met Office, 2011). In contrast, the DD and DN heatwave indices, using the 99th percentile and three consecutive days criteria, provide some evidence about the recurring heatwaves in summer, with

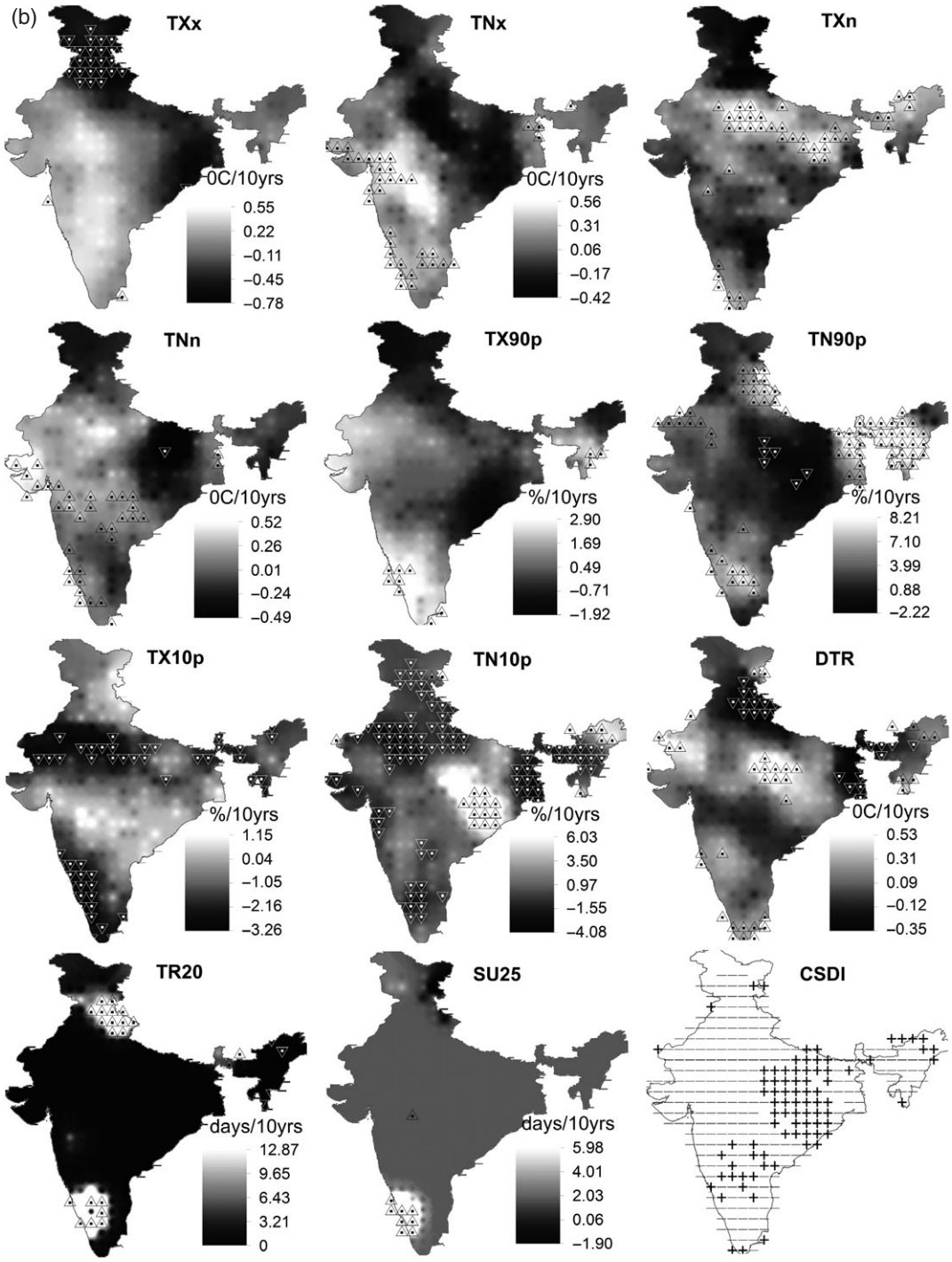

Figure 4. Continued

relatively stronger trends during night-time, consistent with the observed increases in minimum temperature and their extreme indices (Table 2 and Figure 5). Similarly, defining a heatwave as three consecutive days above the 99th percentile, Bumbaco *et al.* (2013) observed an accelerating frequency of night-time heatwaves in Pacific Northwest since the 1990s, in contrast to the general familiarity with daytime heatwaves. Moreover, You *et al.* (2013b) reported an increase in heatwave duration index in China.

In India, the heatwaves in 1991, 1994, 2000, 2002 and 2003 at the regional scales have also led to a large number of human mortality (De *et al.*, 2005, Met Office, 2011), although these events are not captured in the nationally averaged time series, but a noticeable increase can be seen since the 1990s (Figure 5). In general, most of the warmest year along with heatwave episodes has occurred since the 1990s (Füssel, 2009; Met Office, 2011). Figure 6 shows the corresponding changes in the PDF observed in the summer mean and extreme temperature indices during the pre-1990 (i.e. 1971–1989) and

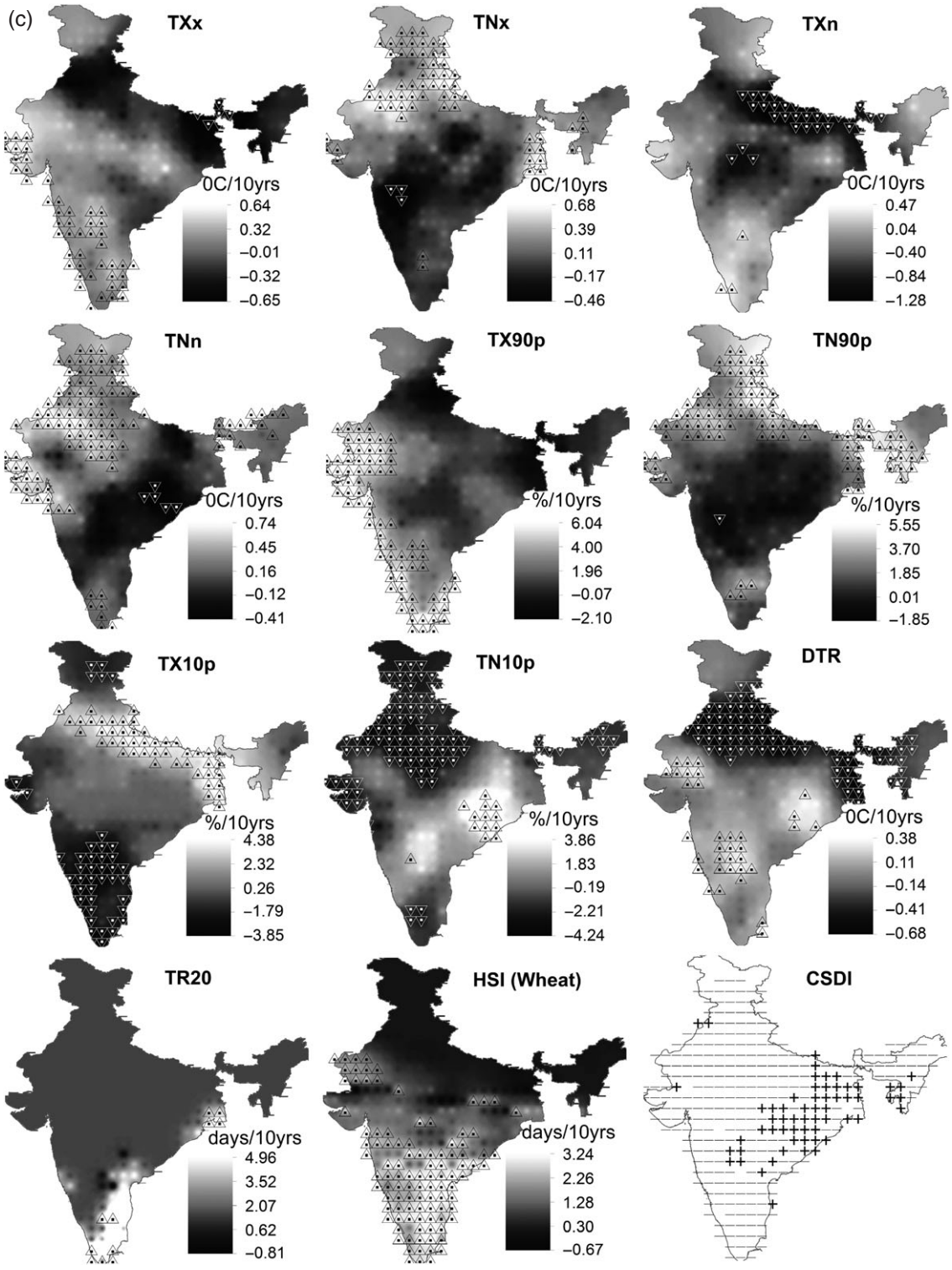

Figure 4. Continued

post-1990 (i.e. 1990–2005) periods, implying an increase in warming tendency during the recent post-1990 phase. However, a close visual inspection indicates that the increases in warm night frequency (TN90p) along with the decreases in cold night frequency (TN10p) have been faster during the post-1990s in comparison with their corresponding daytime indices (Figure 6(b) and (c)). Indeed, the PDF has shifted towards warming trends in most parts of the globe in recent decades, particularly in the frequency of cool and warm nights (Donat and Alexander, 2012). It should also be noted that a little change in mean temperature ($T_{\max}$ and $T_{\min}$) has high impacts on the extreme indices, as observed in the changes in the peaks and tails of distribution (Figure 6). The post-1990 changes in PDF of winter temperature indicate even a faster warming (not shown) over other seasons, possibly

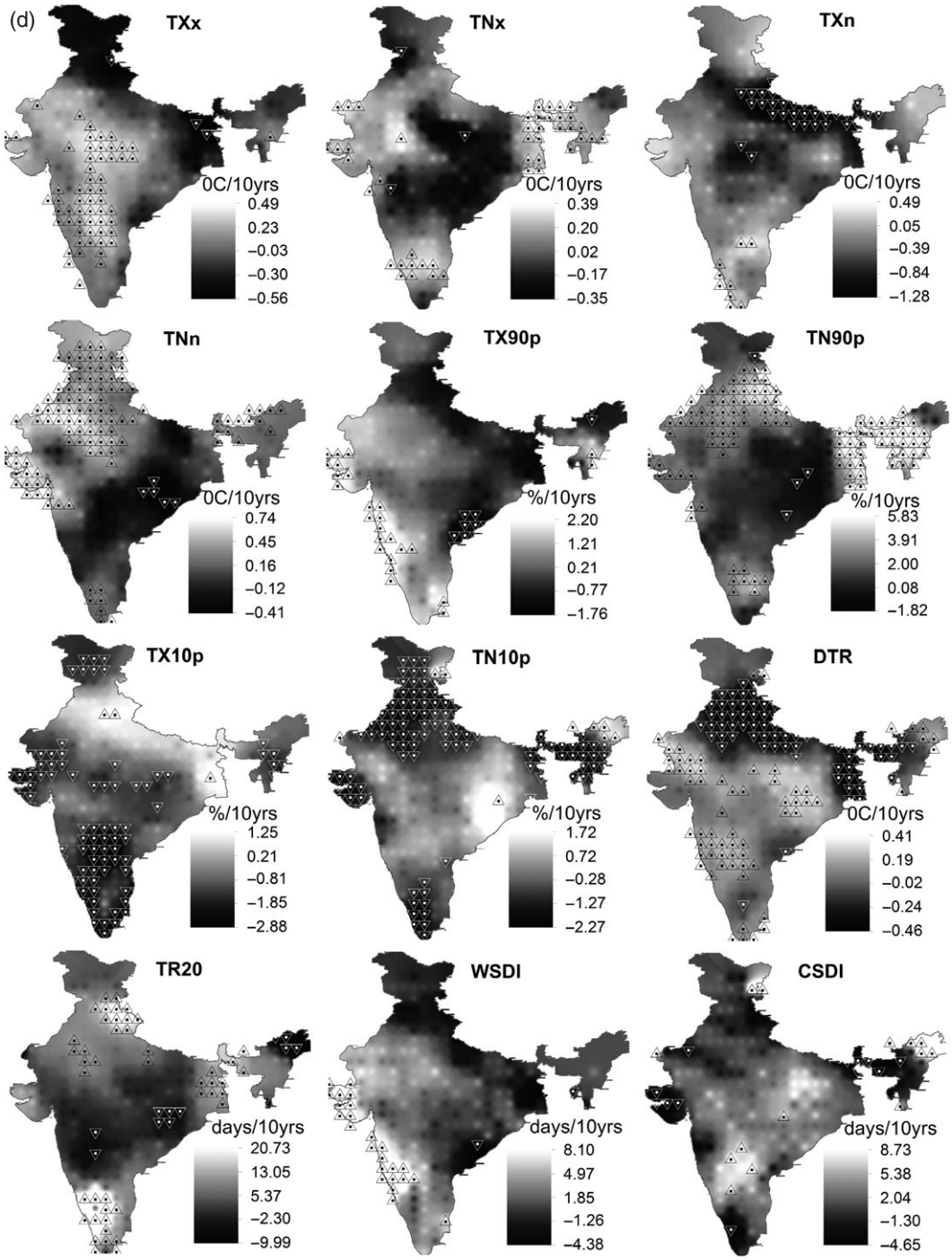

Figure 4. Continued

driving the significant trends for the whole study period as discussed above for different indices.

A relatively cooler night-time temperature acts like a buffer for the human and ecosystems to withstand the daytime heatwaves. The observed significant increases in night-time heatwaves (Figure 5) and their high degree of correspondence with the daytime heatwave indices ($R > 0.8$) appears to have caused the recent human mortality and vulnerability (De *et al.*, 2005, Met Office, 2011), as a high night-time temperature can further exacerbates heatwave conditions (Trigo *et al.*, 2005; Nicholls *et al.*, 2008). A faster rate of warming in night-time temperature ($T_{\min}$) since the 1990s was also reported by Padma Kumari *et al.* (2007) and Kothawale and Rupa Kumar (2005), which resulted in six of the ten warmest years on record in India.

3.2.3. *Changes in DTR and HIS (wheat)*

In contrast to the reported decreasing trends in the mean DTR over most of the areas of the world driven by a larger increase in minimum temperature ($T_{\min}$) (Easterling *et al.*, 1997), we find occurrence of both the

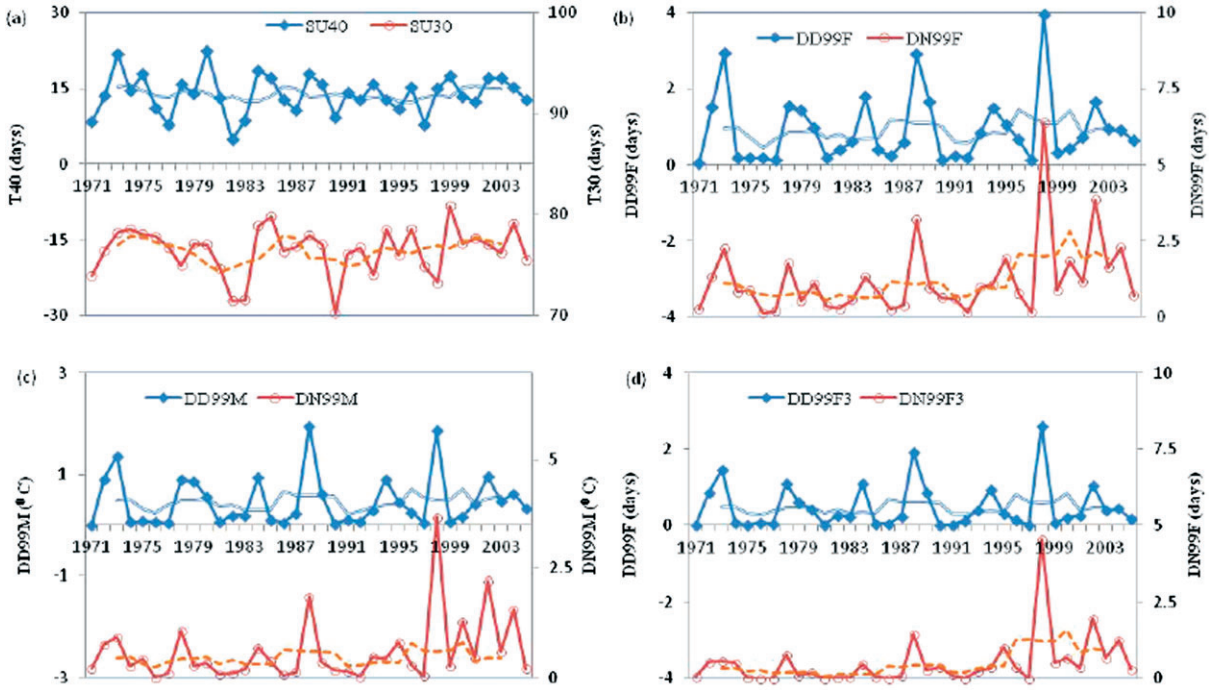

Figure 5. The nationally averaged time series of (a) summer days over 30 and 40 °C (SU30, SU40), (b) degree-day (degree-night) heatwave frequency [$DD_{99}F$ ($DN_{99}F$)], (c) degree-day (degree-night) heatwave magnitude [$DD_{99}M$ ($DN_{99}M$)], (d) degree-day (degree-night) heatwave frequency for three consecutive days [$DD_{99}F3$ ($DN_{99}F3$)]. The inscribed solid and dotted lines indicate the 5-year moving average for the respective indices. A negative scale is used for visual distinction.

increasing and decreasing trends without showing any clear signal of change (Table 2), but similar to the DTR scenario over south Asia (Easterling *et al.*, 1997; Jhajharia and Singh, 2011; Revadekar *et al.*, 2013). It is, however, interesting to observe the spatial consistency of DTR with that of the changes in the mean maximum (T_{max}) and minimum temperature (T_{min}) (Figures 3 and 4). Except for the monsoon season, relatively more significant decreasing trends are found over the north and northeastern parts of India (Figure 4), where T_{min} has decreased significantly (Figure 3). Similarly, the south and western India have experienced more increases in DTR, mainly due to the increases in T_{max}. Overall, the nationally averaged DTR shows a non-significant increasing trend of about 0.08 °C decade^{-1} in summer, winter and annual scales, consistent with the global DTR trend (Alexander *et al.*, 2006).

The HSI index for the winter wheat crop in India indicates pronounced increasing trends across the country except the north and northeastern parts (Table 2 and Figure 4(c)); significantly rising trends are also observed in high proportion. These trends appear to have contributed the heat-induced yield losses of the winter wheat in India (Lobell *et al.*, 2012). Moreover, the spatial pattern of HSI in this study is in agreement with the findings of Teixeira *et al.* (2013) who predicted that a large domain of suitable cropping area of India is under the heat stress risk. Moreover, the observed warming in the mean and extreme indices of minimum temperatures in this study confirms the reduction in the yield of rice due to conspicuous increases in night-time temperature over India and other parts of south Asia (Peng *et al.*, 2004; Welch *et al.*, 2010).

4. The effect of ENSO and SST on the temperature extremes

A comparison of changes in the PDF between the El Niño and La Niña years in the mean and extreme temperature indices indicates that the summer mean minimum and maximum temperature (T_{min} and T_{max}) have decreased in conjunction with the decreases in the warm day and warm night frequency (TX90p and TN90p), and the warmest day and night temperature (TXx and TNx) during the El Niño years in comparison with that during the La Niña years (Figure 7(a)), while the cold day and cold night frequency (TX10p and TN10p) do not show clear changes. In contrast, the monsoon season warm extremes (TX90p, TN90p, TXx, TNx) have increased during the El Niño years along with a clear increase in T_{max} and a decrease in TX10p (Figure 7(b)), suggesting a cooler monsoon during the La Niña phase. In winter, although the mean minimum and maximum temperature (T_{min} and T_{max}) displays a marginal increase during the El Niño years, the warm extremes, such as the TX90p, TN90p, TXx and TNx indices, have decreased marginally (Figure 7(c)). In general, the impact of El Niño on the air temperature in India is weak in winter, although it peaks during this season (Chowdary *et al.*, 2013). The seasonal influence of ENSO observed here is

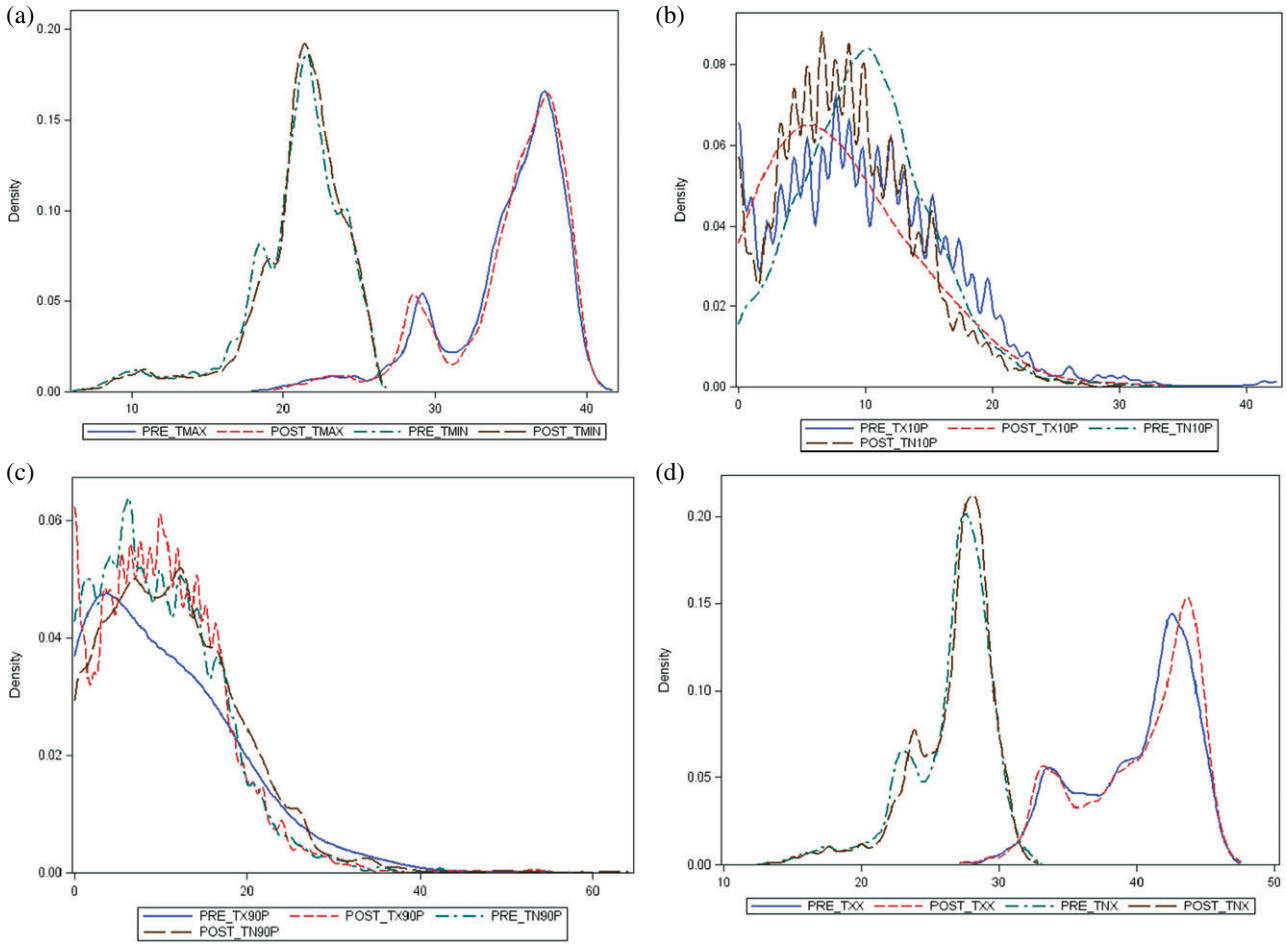

Figure 6. The summer (MAM) season, pre-1990 (i.e. 1971–1989) and post-1990 (i.e. 1990–2005) period, changes in the probability density function (PDF) for the (a) mean temperatures (T_{min} and T_{max}), (b) cold day and night frequency (TX10p, TN10p), (c) warm day and night frequency (TX90p and TN90p) and (d) warmest day and night temperature (TXx and TNx).

consistent with the findings of Revadekar *et al.* (2009), although they observed that an El Niño event leads to an increase in extreme highest temperature during the post-monsoon season (OND). Nicholls *et al.* (2005) reported that the daytime and night-time warm extremes increase substantially in the year after the onset of an El Niño event, as evident from the unusually high heatwave spell and human mortality in 1973, 1988 and 1998 (Figure 5), following the El Niño event of the previous year.

Moreover, the correlation coefficients (R) of the NINO3.4 index (representing the ENSO) of the previous year with the nationally averaged extreme temperature indices of the current year in different seasons indicates that, in summer, the daytime heatwave and warm spell indices (DD99F, DD99F2, DD99F3, WSDI) have significant ($p \leq 0.01$) correlation of about 0.43, while other warm indices (TXx, TX90p, T40) have relatively weak correlation of about 0.39 ($p \leq 0.05$). This suggests a tendency towards the warm extremes in years following an El Niño event. In monsoon, however, a comparatively high degree of correspondence (R 0.62, $p \leq 0.01$) is observed with both daytime and night-time warming extremes, such as the TXx, TX90p, TNx and TN90p indices. For both the summer and monsoon seasons, although the cold day (TX10p), cold night (TN10p) frequency and cold spell duration (CSDI) exhibit anti-correlations with the NINO3.4 index, suggesting decreases following the El Niño events, they are weak and statistically not significant. In winter, the night-time warming, particularly the TNx, TN90p and TR20 indices, tends to increase following the El Niño events as evident from the correlations (R 0.38, $p \leq 0.05$), along with a decreasing tendency in DTR ($R = -0.38$, $p \leq 0.05$). Using the percentile-based extreme temperature indices only, Nicholls *et al.* (2005) and Revadekar *et al.* (2009) also observed similar correspondence with the monthly NINO3.4 index for the east Asia–west Pacific region and the Indian subcontinent.

Chowdary *et al.* (2013) noted that the temperature in India is remotely influenced by the ENSO and locally through the Indian Ocean SST. In particular, the high north Indian Ocean SST, which peaks 3–7 months after the peak in SST over the Niño 3.4 region, results in extreme temperatures and heatwaves primarily due to latent heat release (Trenberth and Fasullo, 2012). In summer, we also find a higher degree of correspondence

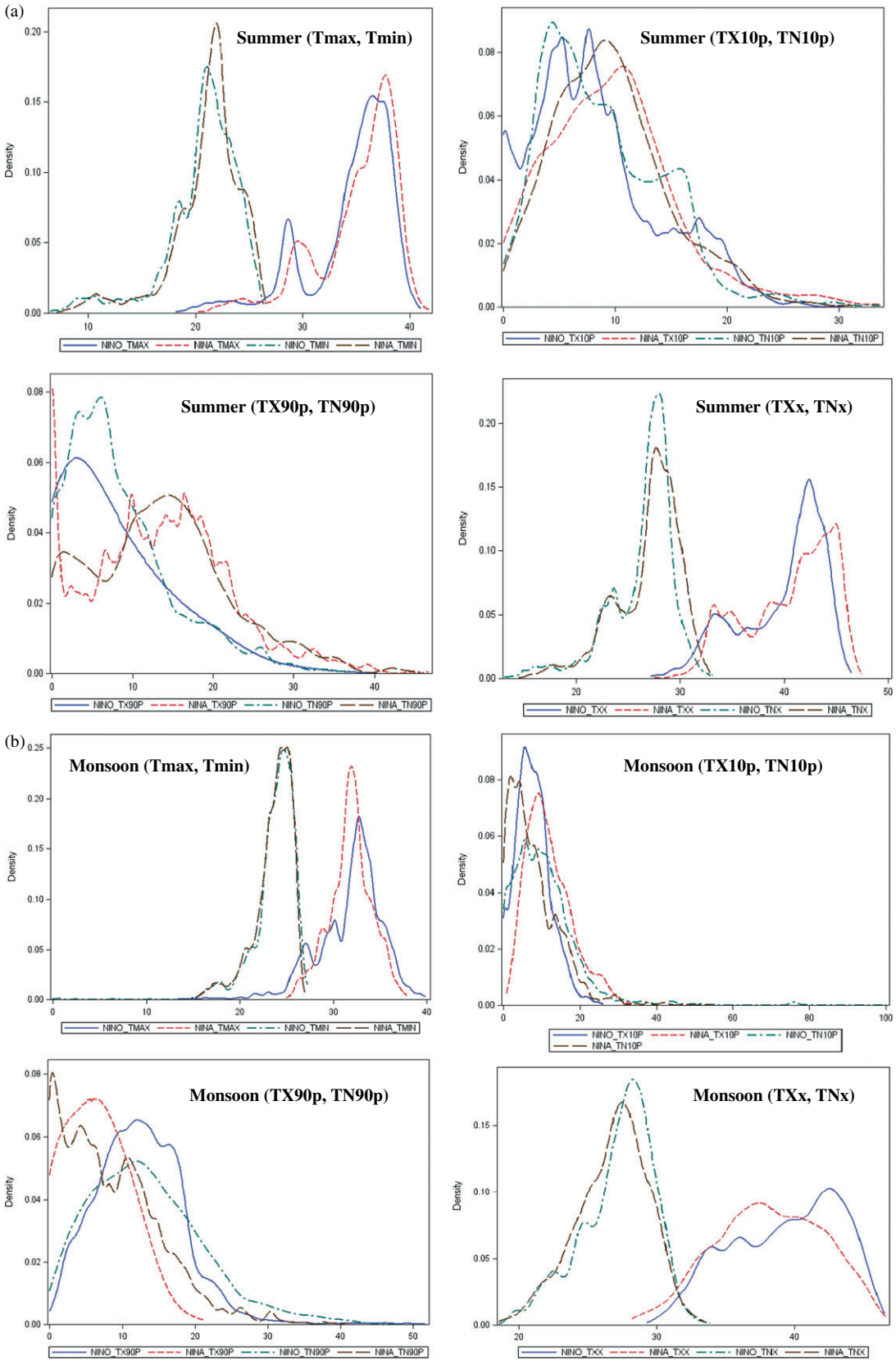

Figure 7. The changes in the probability density function (PDF) for the mean temperatures (T_{min} and T_{max}), cold day and night frequency (TX10p and TN10p), warm day and night frequency (TX90p and TN90p) and warmest day and night temperature (TXx and TNx) between the El Niño and La Niña years in (a) summer (MAM), (b) monsoon (JJAS) and (c) winter seasons during the study period.

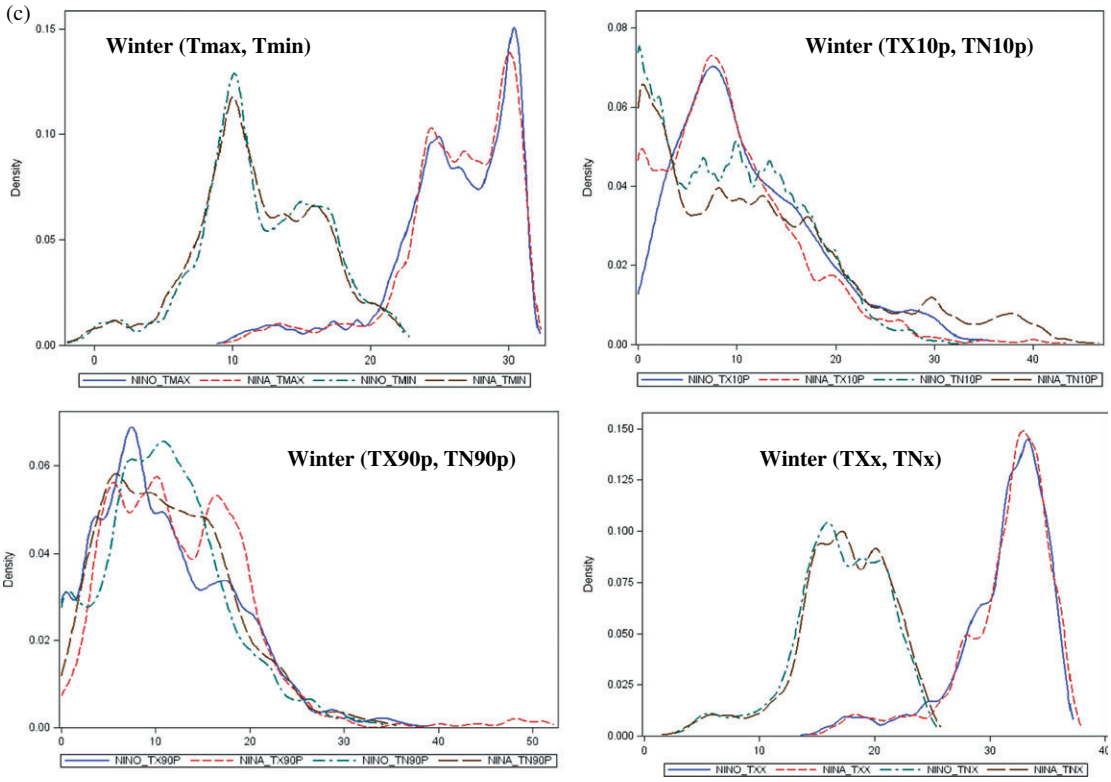

Figure 7. Continued

between the north Indian Ocean SST and the DD and DN heatwave indices in concurrent years, with significant ($p \leq 0.01$) correlation coefficients ranging from 0.41 to 0.56. Moreover, other warming indices (i.e. TXx, TX90p, TNx, TN90p and WSDI) also tend to increase with the increases in the north Indian Ocean SST, having relatively weak correlation coefficients ranging from 0.31 to 0.39. Noteworthy, however, is the concurrence of strong heatwaves in 1973, 1988 and 1998 in India and the anomalously high north Indian Ocean SST (time series not shown). Our results suggest that it is feasible to predict the heatwaves in the summer season from the previous year NINO3.4 index and the current year north Indian Ocean SST, to which both the human society and ecosystems are highly vulnerable.

5. Conclusions

We present the spatiotemporal changes in the mean and extreme temperatures of India using a broad range of indices during 1971–2005. The results provide evidence for an increase in extreme temperatures in terms of decreases in cold extremes and increases in warm extremes in most parts of the Indian subcontinent, generally consistent with the findings of previous studies at the global scale (Alexander *et al.*, 2006; Brown *et al.*, 2008; Field *et al.*, 2012; Donat *et al.*, 2013a) and also with those of the reported trends for the Asian continent (Klein Tank *et al.*, 2006; Caesar *et al.*, 2011). In particular, the winter season is warming at a faster rate in comparison with other seasons, while trends in minimum temperature extremes have been more rapid than trends in maximum temperature extremes, similar to the recent findings of You *et al.* (2013b) for the adjacent country China. Although attribution of these trends is beyond the scope of this research, literature shows the effect of an amplified radiative forcing of greenhouse gas due to relatively less amount of water vapour in the air in winter over other seasons (Aguilar *et al.*, 2009). Similarly, a relatively weak warming in monsoon could be due to the modulation of air temperature from green revolution-induced irrigation and agriculture activity (Roy *et al.*, 2007). Moreover, as expected under the climate change scenario in large parts of the world (IPCC, 2007; Perkins *et al.*, 2012), the observed increases in DD and DN heatwave indices provide evidence about the Indian subcontinent.

Although most of the warm extreme indices are significantly correlated with the ENSO variability, the frequency and spatial extent of the observed warming suggest that the larger part of trends and variability are due to the anthropogenic forcing mechanisms. Both the global and regional climate model simulations have also predicted similar changes in temperature under elevated greenhouse gas and aerosol emission (Rupa Kumar *et al.*, 2006; Kharin *et al.*, 2007), although the observed spatial and seasonal pattern of trends in this study may not be simulated, as indicated by Alexander and Arblaster (2009) for the Australian climate. Since economic liberalization of the 1990s, the Indian subcontinent achieved

a dramatic economic growth characterized by a rapid urbanization, carbon-intensive industrialization and other land-use changes, while the country also experienced more climate extremes with more vulnerable population (Philander, 2012). Consistently, we also find an increased rate of warming and heatwave occurrence since the 1990s. In order to safeguard the increased agricultural vulnerability and the emerging food insecurity under the warming scenarios (Lobell *et al.*, 2012; Wheeler and von Braun, 2013), the spatial delineation of trends in this study can be used for mitigation and adaptation strategies. Future research should focus on the response of the hydrological cycle to the changing patterns of temperature extremes at the sub-regional scales, as water is going to be the critical input for the sustenance of a populous country like India.

Acknowledgements

The authors greatly appreciate the suggestions of the reviewers and the editor for the improvement of the manuscript. The authors are thankful to the Indian Council of Agricultural Research (ICAR), New Delhi, for providing the grant to carry out this research work.

References

Aguilar E, Aziz Barry A, Brunet M, Ekang L, Fernandes A, Massoukina M, Mbah J, Mhanda A, do Nascimento DJ, Peterson TC, Thamba Umba O, Tomou M, Zhang X. 2009. Changes in temperature and precipitation extremes in western central Africa, Guinea Conakry, and Zimbabwe, 1955–2006. *J. Geophys. Res. Atmos.* **114**: D02115, DOI: 10.1029/2008JD011010.

Alexander LV, Arblaster JM. 2009. Assessing trends in observed and modelled climate extremes over Australia in relation to future projections. *Int. J. Climatol.* **29**: 417–435.

Alexander LV, Zhang X, Peterson TC, Caesa J, Gleason B, Klein Tank AMG, Haylock M, Collins D, Trewin B, Rahimzadeh F, Tagipour A, Rupa Kumar K, Revadekar J, Griffiths G, Vincent L. 2006. Global observed changes in daily climate extremes of temperature and precipitation. *J. Geophys. Res. Atmos.* **111**: D05109, DOI: 10.1029/2005jd006290.

Arblaster JM, Alexander LV. 2012. The impact of the El Niño-Southern Oscillation on maximum temperature extremes. *Geophys. Res. Lett.* **39**: L20702, DOI: 10.1029/2012GL053409.

Auffhammer M, Ramanathan V, Vincent JR. 2012. Climate change, the monsoon, and rice yield in India. *Clim. Change* **111**: 411–424, DOI: 10.1007/s10584-011-0208-4.

Bhutiyani MR, Kale VS, Pawar NJ. 2007. Long-term trends in maximum, minimum and mean annual air temperatures across the northwestern Himalaya during the twentieth century. *Clim. Change* **85**: 159–177.

Bolch T, Kulkarni A, Kääb A, Huggel C, Paul F, Cogley JG, Frey H, Kargel JS, Fujita K, Scheel M, Bajracharya S, Stoffel M. 2012. The state and fate of Himalayan glaciers. *Science* **336**, DOI: 10.1126/science.1215828.

Brown SJ, Caesar J, Ferro CAT. 2008. Global changes in extreme daily temperature since 1950. *J. Geophys. Res. Atmos.* **113**: D05115, DOI: 10.1029/2006jd008091.

Bumbaco KA, Dello KD, Bond NA. 2013. History of Pacific Northwest heat waves: synoptic pattern and trends. *J. Appl. Meteorol. Climatol.* **52**: 1618–1631, DOI: 10.1175/JAMC-D-12-094.1.

Caesar J, Alexandar L, Russell V. 2006. Large-scale changes in observed daily maximum and minimum temperatures: creation and analysis of a new gridded data set. *J. Geophys. Res. Atmos.* **111**: DO5101, DOI: 10.1029/2005JD006280.

Caesar J, Alexander LV, Trewin B, Tse-ring K, Sorany L, Vuniyayawa V, Keosavang N, Shimana A, Htay MM, Karmacharya J. 2011. Changes in temperature and precipitation extremes over the Indo-Pacific region from 1971 to 2005. *Int. J. Climatol.* **31**: 791–801, DOI: 10.1002/joc.2118.

Chandler RE, Scott EM. 2011. *Statistical Methods for Trend Detection and Analysis in the Environmental Sciences*. Wiley: Chichester, UK.

Chowdary JS, John N, Gnanaseelan C. 2013. Interannual variability of surface air-temperature over India: impact of ENSO and Indian Ocean sea surface temperature. *Int. J. Climatol.*, DOI: 10.1002/joc.3695.

Christy JR, Norris WB, McNider RT. 2008. Surface temperature variations in East Africa and possible causes. *J. Clim.* **22**: 3342–3356.

Daly C. 2006. Guidelines for assessing the suitability of spatial climate data sets. *Int. J. Climatol.* **26**: 707–721.

Dash SK, Mamgain A. 2011. Changes in the frequency of different categories of temperature extremes in India. *J. Appl. Meteorol. Climatol.* **50**: 1842–1858.

De US, Dube RK, Prakasa Rao GS. 2005. Extreme weather events over India in the last 100 years. *J. Indian Geophys. Union* **9**: 173–187.

De US, Mukhopadhyay RK. 1998. Severe heat wave over Indian subcontinent in 1998 in a perspective of global Climate. *Curr. Sci*. **75**: 1308–1311.

Dey S, Tripathi SN. 2008. Aerosol direct radiative effects over Kanpur in the Indo-Gangetic basin, northern India: long-term (2001–2005) observations and implications to regional climate. *J. Geophys. Res. Atmos.* **113**: D04212, DOI: 10.1029/2007JD009029.

Dinpashoh Y, Mirabbasi R, Jhajharia D, Abianeh HZ, Mostafaeipour A. 2013. Effect of short term and long-term persistence on identification of temporal trends. *J. Hydrol. Eng.*, DOI: 10.1061/(ASCE)HE.1943-5584.0000819.

Donat MG, Alexander LV. 2012. The shifting probability distribution of global daytime and night-time temperatures. *Geophys. Res. Lett.* **39**: L14707, DOI: 10.1029/2012GL052459.

Donat MG, Alexander LV, Yang H, Durre I, Vose R, Dunn RJH, Willett KM, Aguilar E, Brunet M, Caesar J, Hewitson B, Jack C, Klein Tank AMG, Kruger AC, Marengo J, Peterson TC, Renom M, Oria Rojas C, Rusticucci M, Salinger J, Elrayah AS, Sekele SS, Srivastava AK, Trewin B, Villarroel C, Vincent LA, Zhai P, Zhang X, Kitching S. 2013a. Updated analyses of temperature and precipitation extreme indices since the beginning of the twentieth century: the HadEX2 dataset. *J. Geophys. Res. Atmos.* **118**: 2098–2118, DOI: 10.1002/jgrd.50150.

Donat MG, Peterson TC, Brunet M, King D, Almazroui M, Kolli RK, Boucherf D, Al-Mulla AY, Nour AY, Aly AA, Nada TAA, Semawi MM, Abdullah H, Dashti A, Salhab TG, El Fadli KI, Muftah MK, Eida SD, Badi W, Driouech F, El Rhaz K, Abubaker MJY, Ghulam AS, Erayah AS, Mansour MB, Alabdouli WO, Al Dhanhani JS, Al Shekaili MN. 2013b. Changes in extreme temperature and precipitation in the Arab region: long-term trends and variability related to ENSO and NAO. *Int. J. Climatol.*, DOI: 10.1002/joc.3707.

Easterling DR, Horton B, Jones PD, Peterson TC, Karl TR, Parker DE, Salinger M, Razuvayev V, Plummer N, Jamason P, Folland CK. 1997. Maximum and minimum temperature trends for the globe. *Science* **277**: 364–367.

Easterling DR, Meehl GA, Parmesan C, Changnon SA, Karl TR, Mearns LO. 2000. Climate extremes: observations, modeling, and impacts. *Science* **289**(5487): 2068–2074.

Field CB, Barros V, Stocker TF, Qin D, Dokken DJ, Ebi KL, Mastrandrea MD, Mach KJ, Plattner G-K, Allen SK, Tignor M, Midgley PM (eds). 2012. *Intergovernmental Panel on Climate Change: Managing the Risks of Extreme Events and Disasters to Advance Climate Change Adaptation*. Cambridge University Press: Cambridge, UK.

Fowler HJ, Archer DR. 2006. Conflicting signals of climate change in the upper Indus basin. *J. Clim.* **19**: 4276–4293.

Füssel H-M. 2009. An updated assessment of the risks from climate change based on research published since the IPCC Fourth Assessment Report. *Clim. Change* **97**: 469–482, DOI: 10.1007/s10584-009-9648-5.

Gershunov A, Cayan DR, Iacobellis SF. 2009. The great 2006 heat wave over California and Nevada: signal of an increasing trend. *J. Clim.* **22**: 6181–6203.

Goswami BN, Venugopal V, Sengupta D, Madhusoodanan MS, Xavier PK. 2006. Increasing trend of extreme rain events over India in a warming environment. *Science* **314**: 1442–1445.

Halpert MS, Ropelewski CF. 1992. Surface temperature patterns associated with the Southern Oscillation. *J. Clim.* **5**: 557–593.

Hipel KW, McLeod AI. 2005. *Time Series Modeling of Water Resources and Environmental Systems*. Elsevier: Amsterdam. http://www.stats.uwo.ca/faculty/aim/1994Book/.

Hoyos CD, Agudelo PA, Webster PJ, Curry JA. 2006. Deconvolution of the factors contributing to the increase in global hurricane intensity. *Science* **312**: 94–97.

IPCC. 2007. Climate change 2007: The physical science basis. In *Contribution of Working Group I to the Fourth Assessment Report of the Intergovernmental Panel on Climate Change*, Solomon S, Qin D, Manning M, Chen Z, Marquis M, Averyt KB, Tignor M, Miller HL (eds). Cambridge University Press: New York, NY, p 996.

Jhajharia D, Singh VP. 2011. Trends in temperature, diurnal temperature range and sunshine duration in northeast India. *Int. J. Climatol.* **31**: 1353–1367, DOI: 10.1002/joc.2164.

Jhajharia D, Yadav BK, Maske S, Chattopadhyay S, Kar AK. 2012. Identification of trends in rainfall, rainy days and 24 h maximum rainfall over subtropical Assam in northeast India. *C. R. Geosci.* **344**: 1–13.

Jhajharia D, Dinpashoh Y, Kahya E, Choudhary RR, Singh VP. 2013. Trends in temperature over Godavari River basin in Southern Peninsular India. *Int. J. Climatol.* , DOI: 10.1002/joc.3761.

Kharin VV, Zhang X, Hegerl GC. 2007. Changes in temperature and precipitation extremes in the IPCC ensemble of global coupled model simulations. *J. Clim.* **20**: 1419–1444, DOI: 10.1175/JCLI4066.1.

Kiktev D, Sexton DMH, Alexander L, Folland CK. 2003. Comparison of modeled and observed trends in indices of daily climate extremes. *J. Clim*. **16**: 3560–3571.

Klein Tank AMG, Können GP. 2003. Trends in indices of daily temperature and precipitation extremes in Europe, 1946–1999. *J. Clim.* **16**: 3665–3680.

Klein Tank AMG, Peterson TC, Quadir DA, Dorji S, Zou X, Tang H, Santhosh K, Joshi UR, Jaswal AK, Kolli RK, Sikder A, Deshpande NR, Revadekar JV, Yeleuova K, Vandasheva S, Faleyeva M, Gomboluudev P, Budhathoki KP, Hussain A, Afzaal M, Chandrapala L, Anvar H, Amanmurad D, Asanova VS, Jones PD, New MG, Spektorman T. 2006. Changes in daily temperature and precipitation extremes in central and south Asia. *J. Geophys. Res. Atmos.* **111**: D16105, DOI: 10.1029/2005JD006316.

Kothawale DR, Rupa Kumar K. 2005. On the recent changes in surface temperature trends over India. *Geophys. Res. Lett.* **32**: L18714, DOI: 10.1029/2005GL023528.

Kothawale DR, Munot AA, Borgaonkar HP. 2008. Temperature variability over Indian Ocean and its relationship with Indian summer monsoon rainfall. *Theor. Appl. Climatol.* **9**(2): 31–45.

Kothawale DR, Munot AA, Krishna KK. 2010. Surface air temperature variability over India during 1901–2007, and its association with ENSO. *Clim. Res.* **42**: 89–104, DOI: 10.3354/cr00857.

Krishna Kumar K, Kamala K, Rajagopalan B, Hoerling MP, Eischeid JK, Patwardhan SK, Srinivasan G, Goswami BN. 2011. The once and future pulse of Indian monsoonal climate. *Clim. Dyn.* **36**: 2159–2170, DOI: 10.1007/s00382-010-0974-0.

Krishnamurthy CKB, Lall U, Kwon H-H. 2009. Changing frequency and intensity of rainfall extremes over India from 1951 to 2003. *J. Clim.* **22**, DOI: 10.1175/2009JCLI2896.1.

Krishnan R, Ramanathan V. 2002. Evidence of surface cooling from absorbing aerosols. *Geophys. Res. Lett.* **29**: 1340, DOI: 10.1029/2002GL014687.

Lobell DB, Sibley A, Ortiz-Monasterio JI. 2012. Extreme heat effects on wheat senescence in India. *Nat. Clim. Change* **2**: 186–189.

May W. 2011. The sensitivity of the Indian summer monsoon to a global warming of 2 °C with respect to pre-industrial times. *Clim. Dyn.* **37**: 1843–1868.

Met Office. 2011. *Climate: Observations, Projections and Impacts*. Met Office: Exeter, UK. http://www.metoffice.gov.uk/media/pdf/7/i/India.pdf.

Morak S, Hegerl GC, Christidis N. 2013. Detectable changes in the frequency of temperature extremes. *J. Clim*. **26**: 1561–1574, DOI: 10.1175/JCLI-D-11-00678.1.

New MG, Hulme M, Jones PD. 2000. Representing twentieth century space-time climate variability. Part II: Development of 1901–96 monthly grids of terrestrial surface climate. *J. Clim.* **13**: 2217–2238.

Nicholls N, Baek HJ, Gosai A, Chambers LE, Choi Y, Collins D, Della-Marta PM, Griffiths GM, Haylock MR, Lata R, Maitrepierre L, Manton MJ, Nakamigawa H, Ouprasitwong N, Solofa D, Thuy DT, Tibig L, Trewin B, Vediapan K, Zhai P. 2005. The El Niño-Southern Oscillation and daily temperature extremes in east Asia and the west Pacific. *Geophys. Res. Lett.* **32**: L16714, DOI: 10.1029/2005GL022621.

Nicholls N, Skinner C, Loughnan N, Tapper N. 2008. A simple heat alert system for Melbourne, Australia. *Int. J. Biometeorol.* **52**: 375–384, DOI: 10.1007/s00484-007-0132-5.

Padma Kumari B, Londhe AL, Daniel S, Jadhav DB. 2007. Observational evidence of solar dimming: Offsetting surface warming over India. *Geophys. Res. Lett*. **34**: L21810, DOI:10.1029/2007GL031133.

Pai DS, Thapliyal V, Kokate PD. 2004. Decadal variation in the heat and cold waves over India during 1971–2000. *Mausam* **55**: 281–292.

Peng S, Huang J, Sheehy JE, Laza RC, Visperas RM, Zhong X, Centeno GS, Khush GS, Cassman KG. 2004. Rice yields decline with higher night temperature from global warming. *Proc. Natl. Acad. Sci. USA* **101**: 9971–9975.

Perkins SE, Alexander LV. 2013. On the measurement of heat waves. *J. Clim.* **26**: 4500–4570, DOI: 10.1175/JCLI-D-12-00383.1.

Perkins SE, Alexander LV, Nairn J. 2012. Increasing frequency, intensity and duration of observed global heat waves and warm spells. *Geophys. Res. Lett.* **39**: L20714, DOI: 10.1029/2012GL053361.

Peterson TC, Manton MJ. 2008. Monitoring changes in climate extremes: a tale of international collaboration. *Bull. Am. Meteorol. Soc.* **89**: 1266–1271, DOI: 10.1175/2008BAMS2501.1.

Philander SG. 2012. *Encyclopedia of Global Warming and Climate Change*, Vol. **1**, 2nd edn. SAGE Publications: California, CA. ISBN: 978.1.41299261.9.

Pingale SM, Khare D, Jat MK, Adamowski J. 2014. Spatial and temporal trends of mean and extreme rainfall and temperature for the 33 urban centers of the arid and semi-arid state of Rajasthan, India. *Atmos. Res.* **138**: 73–90.

Revadekar JV, Kothawale DR, Rupa Kumar K. 2009. Role of El Niño/La Niña in temperature extremes over India. *Int. J. Climatol.* **29**: 2121–2129.

Revadekar JV, Hameed S, Collins D, Manton M, Sheikh M, Borgaonkar HP, Kothawale DR, Adnan M, Ahmed AU, Ashraf J, Baidya S, Islam N, Jayasinghearachchi D, Manzoor N, Premalal KHMS, Shreshta ML. 2013. Impact of altitude and latitude on changes in temperature extremes over South Asia during 1971–2000. *Int. J. Climatol.* **33**: 199–209.

Roy SS, Mahmood R, Niyogi D, Lei M, Foster SA, Hubbard KG, Douglas E, Pielke R Sr. 2007. Impacts of the agricultural Green Revolution–induced land use changes on air temperatures in India. *J. Geophys. Res.* **112**: D21108, DOI: 10.1029/2007JD008834.

Rupa Kumar K, Krishna Kumar K, Pant GB. 1994. Diurnal asymmetry of surface temperature trends over India. *Geophys. Res. Lett.* **21**(8): 677–680.

Rupa Kumar K, Sahai AK, Krishnakumar K, Patwardhan SK, Mishra PK, Revadekar JV, Kamala K, Pant GB. 2006. High-resolution climate change scenarios for India for the 21st century. *Curr. Sci.* **90**(3): 334–345.

Santo FE, de Lima MIP, Ramos AM, Trigo RM. 2013. Trends in seasonal surface air temperature in mainland Portugal, since 1941. *Int. J. Climatol.*, DOI: 10.1002/joc.3803.

Sen PK. 1968. Estimates of the regression coefficient based on Kendall's tau. *J. Am. Stat. Assoc.* **63**: 1379–1389, DOI: 10.1080/01621459.1968.10480934.

Shakoor H, Armstrong BG, Gouveia N, Wilkinson P. 2005. Mortality displacement of heat-related deaths: a comparison of Delhi, Sao Paulo, and London. *Epidemiology* **16**: 613–620.

Shepard D. 1968. A two-dimensional interpolation function for irregularly-spaced data. In *Proceedings of the 23rd National Conference Association for Computing Machinery*. ACM (ed). ACM: 517–524.

Singh P, Kumar V, Thomas T, Arora M. 2008. Basin-wide assessment of temperature trends in northwest and central India. *Hydrol. Sci. J.* **53**(2): 421–433.

Smith TM, Reynolds RW, Peterson TC, Lawrimore J. 2008. Improvements to NOAA's historical merged land-ocean surface temperature analysis (1880–2006). *J. Clim.* **21**: 2283–2296.

Srivastava AK, Rajeevan M, Kshirsagar SR. 2009. Development of a high resolution daily gridded temperature data set (1969–2005) for the Indian region. *Atmos. Sci. Lett.* **10**: 249–254.

Teixeira E, Fischer G, van Velthuizen H, Walter C, Ewert F. 2013. Global hot-spots of heat stress on agricultural crops due to climate change. *Agric. For. Meteorol.* **170**: 206–215.

Trenberth KE, Fasullo JT. 2012. Climate extremes and climate change: the Russian heat wave and other climate extremes of 2010. *J. Geophys. Res.* **117**: D17103, DOI: 10.1029/2012JD018020.

Trigo R, Garia-Herrera R, Diaz J, Trigo I, Valente M. 2005. How exceptional was the early August 2003 heatwave in France? *Geophys. Res. Lett.* **32**: L10701, DOI: 10.1029/.

Unnikrishnan AS, Shankar D. 2007. Are sea-level-rise trends along the coasts of the north Indian Ocean consistent with global estimates? *Glob. Planet. Change* **57**: 301–307.

Vincent LA, Aguilar E, Saindou M, Hassane AF, Jumaux G, Roy D, Booneeady P, Virasami R, Randriamarolaza LYA, Faniriantsoa FR, Amelie V, Seeward H, Montfraix B. 2011. Observed trends in indices of daily and extreme temperature and precipitation for the countries of the western Indian Ocean, 1961–2008. *J. Geophys. Res. Atmos.* **116**: D10108, DOI: 10.1029/2010 JD015303.

Vörösmarty CJ, McIntyre PB, Gessner MO, Dudgeon D, Prusevich A, Green P, Glidden S, Bunn SE, Sullivan CA, Liermann CR, Davies PM. 2010. Global threats to human water security and river biodiversity. *Nature* **467**: 555–561.

Vose RS, Easterling DR, Gleason B. 2005. Maximum and minimum temperature trends for the globe: an update through 2004. *Geophys. Res. Lett.* **32**: L23822, DOI: 10.1029/2005GL024379.

Welch JR, Vincent JR, Auffhammer M, Moya PF, Dobermann A, Dawe D. 2010. Rice yields in tropical/subtropical Asia exhibit large but opposing sensitivities to minimum and maximum temperatures. *Proc. Natl. Acad. Sci. USA* **107**(33): 14562–14567.

Wheeler T, von Braun J. 2013. Climate change impacts on global food security. *Science* **341**: 508–513.

World Bank. 2013. Turn down the heat: climate extremes, regional impacts and the case for resilience. A report for the World Bank by the Potsdam Institute for Climate Impact Research and Climate Analytics. World Bank: Washington, DC.

You QL, Kang SC, Aguilar E, Pepin N, Fluegel WA, Yan YP. 2011. Changes in daily climate extremes in China and their connection to the large scale atmospheric circulation during 1961–2003. *Clim. Dyn.* **36**: 2399–2417, DOI: 10.1007/s00382-009-0735-0.

You Q, Fraedrich K, Min J, Kang S, Zhu X, Ren G, Meng X. 2013a. Can temperature extremes in China be calculated from reanalysis? *Glob. Planet. Change* **111**: 268–279.

You Q, Fraedrich K, Sielmann F, Min J, Kang S, Ji Z, Zhu X, Ren G. 2013b. Present and projected degree days in China from observation, reanalysis and simulations. *Clim. Dyn.* , DOI: 10.1007/s00382-013-1960-0.

Zhang X, Alexander LV, Hegerl GC, Jones P, Klein Tank A, Peterson TC, Trewin B, Zwiers FW. 2011. Indices for monitoring changes in extremes based on daily temperature and precipitation data. *WIREs Clim. Change* **2**(6): 851–870, DOI: 10.1002/wcc.147.

